Norwegian Meteorological Institute

No. 2/2021
ISSN 2387-4201
Oceanography

METreport

NorKyst800 model currents validation

Comparison of modeled currents with primitive ship data and ADCP data

Nils Melsom Kristensen and Yvonne Gusdal

Norwegian Meteorological Institute

METreport

Title	Date
NorKyst800 model currents validation	May 3, 2021
Section	**Report no.**
Ocean and Ice	2/2021
Author(s)	**Classification**
Nils Melsom Kristensen and Yvonne Gusdal	● Free ○ Restricted
Client(s)	**Client's reference**
Norwegian Research Council – by Project owner Kongsberg Maritime	PNO 282385

Abstract

We have used data like speed through water, speed over ground, course and position from the ship Samskip Kvitbjørn to investigate whether such primitive ship data may be used to assess model predictions of currents derived by our ocean model NorKyst800. Since the primitive ship data do not provide us with true current speed and direction, a conversion method is proposed. Using this method we compare all the available ship data with modeled currents. We find that their statistical distributions regarding current speed are very similar, which suggests that the method is useful. To assess the quality of the NorKyst800 model, and the proposed conversion method of primitive ship data, we also include a more traditional comparison with ADCP moorings for a smaller area in the north-western part of Norway. The area of the current moorings was also regularly passed by the ship Samskip Kvitbjørn, so in parts of the work we limit the area of analysis to the same geographical area as where the ADCP moorings were located. The results are encouraging in that the statistical distributions of currents based on all the three sources are similar. This in turn suggests that comparing model current speed with primitive ship data may be useful for evaluating the quality of the modeled currents. Thus, we conclude that the developed method has the potential of giving us access to a very large amount of hitherto unused sources of observations of currents. In turn this may be used to provide further estimates of the quality of the near surface currents derived from our ocean models. This requires, however, that the user is aware of and understands the possible sources of error the method has, and its limited degree of accuracy.

Keywords

ROMS, NorKyst800, validation, currents

Disciplinary signature	Responsible signature
Lars Petter Røed	Kai H. Christensen

Abstract

We have used data like speed through water, speed over ground, course and position from the ship Samskip Kvitbjørn to investigate whether such primitive ship data may be used to assess model predictions of currents derived by our ocean model NorKyst800. Since the primitive ship data do not provide us with true current speed and direction, a conversion method is proposed. Using this method we compare all the available ship data with modeled currents. We find that their statistical distributions regarding current speed are very similar, which suggests that the method is useful. To assess the quality of the NorKyst800 model, and the proposed conversion method of primitive ship data, we also include a more traditional comparison with ADCP moorings for a smaller area in the north-western part of Norway. The area of the current moorings was also regularly passed by the ship Samskip Kvitbjørn, so in parts of the work we limit the area of analysis to the same geographical area as where the ADCP moorings were located. The results are encouraging in that the statistical distributions of currents based on all the three sources are similar. This in turn suggests that comparing model current speed with primitive ship data may be useful for evaluating the quality of the modeled currents. Thus, we conclude that the developed method has the potential of giving us access to a very large amount of hitherto unused sources of observations of currents. In turn this may be used to provide further estimates of the quality of the near surface currents derived from our ocean models. This requires, however, that the user is aware of and understands the possible sources of error the method has, and its limited degree of accuracy.

Norwegian Meteorological Institute
Org.no 971274042
post@met.no
www.met.no / www.yr.no

Oslo
P.O. Box 43, Blindern
0313 Oslo, Norway
T. +47 22 96 30 00

Bergen
Allégaten 70
5007 Bergen, Norway
T. +47 55 23 66 00

Tromsø
P.O. Box 6314, Langnes
9293 Tromsø, Norway
T. +47 77 62 13 00

Contents

1 Introduction

1.1 Background

As a part of the InnoCurrent project, MET Norway should get access to high quality observations of ocean currents along the Norwegian coast from a newly developed speed-log instrument from the ship Samskip Kvitbjørn. This speed-log instrument is a ship mounted ADCP, and together with information about the ship movement based on GPS this would provide us detailed vertical information about the current speed and direction for large parts of the water column along the ship track. Our task was mainly to do a comparison between the observed currents from the ship mounted ADCP and the simulated currents from the operational ocean model NorKyst800 (*Albretsen et al.*, 2011) so as to assess the quality of the modeled currents. The results from this comparison would in turn be used by other project partners in developing methods whereby route optimization based on forecasts from the NorKyst800 model may be utilized to reduce climate gas emissions from ships. Unfortunately, and due to circumstances outside of our control, the new type of speed-log never became operational. Hence no data from this instrument were made available to us.

1.2 Present research

In an attempt to fulfill our obligations in the project, we were given access to more primitive ship data such as speed through water from a simpler type of speed-log, speed over ground and course over ground from GPS together with the ship's position. By calculating the difference between the speed over ground and the speed trough water we obtain a proxy for the component of the true ocean current along the ship's course along its track. However, it does not give us any information about the true current direction which is necessary to compute the true current speed. Thus a method is put forward (Section 2) that converts the primitive ship data into a true current speed and direction. If the method proves to be useful, primitive ship data may potentially be used as a measure of the true ocean currents. If so we may then make a comparison with ocean currents from the NorKyst800 model.

To assess the usefulness of the method we have used another data set available to us, namely, a number of semi-permanent current measurement from moored ADCPs (Acoustic Doppler Current Profilers) for a limited area on the north-west coast of Norway (hereafter referred to the Sulafjorden area). This data is collected through a measurement campaign within the project "Fergefri E39" (*Furevik et al.*, 2020; *Harstveit et al.*, 2018). The objective of "Fergefri E39" is to monitor the environment with regards to wind, currents, waves etc. for planning and dimensional purposes for a future bridge construction across the Sulafjorden. In addition to the ADCPs the data therefore consists of a large collection of atmospheric and oceanographic parameters. Here we have focused on the moorings containing measurements of currents from ADCPs. We have used these data together with primitive ship data and model output from the same area to assess the usefulness of the developed method to convert the primitive ship data into true current speed and direction (Section 4).

Finally, based on the developed method, we perform a comparison of the currents from NorKyst800 with the ship data from the ship Samskip Kvitbjørn for the entire Norwegian coast as presented in Section 3. A discussion of the results is offered in Section 5, while a summary is put forward in Section 6.

2 Data and method

2.1 The "relative current" (SOG-STW)

The data made available to us was the ship's *speed over ground* (hereafter SOG) and *speed through water* (STW) in addition to the ship's *GPS position* and *course over ground* (COG). No explicit information about the true current speed and direction was provided. To create a proxy for the true current vector we first calculate the difference in SOG and STW. This gives us the current's componet along the ship's travel direction hereafter referred to as the "relative current" or simply SOG-STW (Figure 1). It is emphasized that there are many other factors that may influence the difference between the ship's STW and SOG, e.g., wind, waves and local disturbances around the hull of the ship. These factors are not further discussed in this report, but adds to the uncertainty when calculating the true speed. Also illustrated by Figure 1 is that the information we get is only the component of the true current along the ship's course. It does not give us any information about the true current direction. In Figure 1 the STW is denoted by the big red arrow, and the SOG is denoted by the thinner and shorter blue arrow. This indicates that the STW is larger than the SOG, giving us a negative value of SOG-STW (the black arrow). This is commonly referred to as a case of "sailing against the current", whereas positive values of SOG-STW is commonly referred to as "sailing with the current". However, this way of describing the current as either "with" or "against" is only relevant when the ship is used as the reference frame, and is not very useful when talking about the true or simulated currents. To account for this we also introduce the "relative direction" (hereafter referred to as $course_r$):

$$course_r = \begin{cases} \mathrm{COG} & \text{if SOG-STW} \leq 0, \\ (\mathrm{COG} - 180) & \text{if SOG-STW} > 0, \end{cases} \tag{1}$$

where COG is measured in degrees from 0 to 360. This gives us the absolute speed and direction of the relative current component experienced by the ship for all positions along the ship's track.

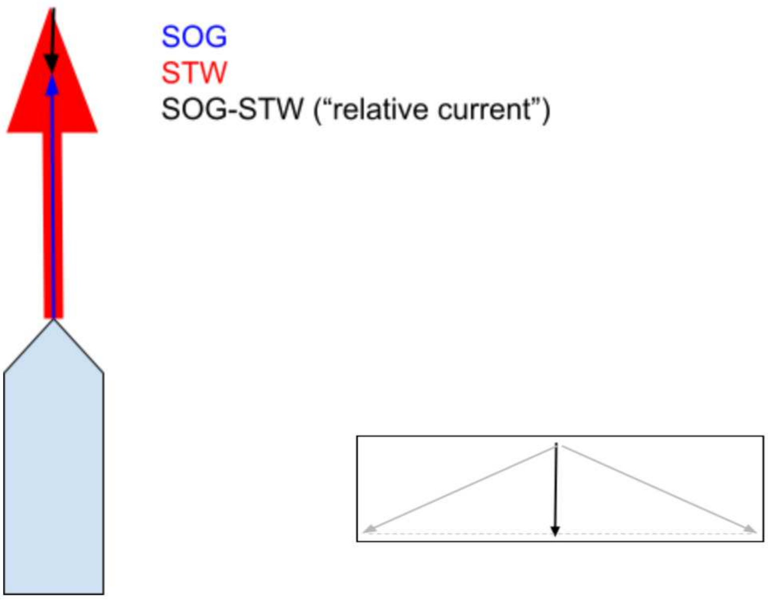

Figure 1: Schematic illustration of how the "relative current" (SOG-STW) is calculated. To the left is the ship and the SOG and STW indicated using arrows. The SOG-STW is the black arrow. Since it points in the opposite direction of the ship's travel direction, it indicates that the ship is "sailing against current". The direction of the SOG-STW arrow is further referred to as the "relative course" ($course_r$). As shown in the bottom right part (inside the black square), the direction of the true current (light grey arrows) could differ quite substantially (actually up to +/- 90 degrees) from the relative current direction. Moreover, the true current speed is always equal to or higher than the relative current speed.

2.2 Filtering of the ship data

To remove as much "bad data" as possible we first (Filter 0) remove all ship data where SOG is *less* than 10 knots. The rationale for setting a lower limit of speed for the ship is to filter out all the data where the ship do significant maneuvering, which would have a big impact on the SOG-STW calculation. Thus, this choice is kind of arbitrary and may have been chosen to be higher or lower, that might or might not have an impact on the results. The latter has not been tested in the present study. Next we remove all data with a relative current speed exceeding 2 m/s (Filter 1).

As explained, the ship data does not provide explicit information about the true currents. To obtain a proxy for the true currents, which then enables us to compare observed and modeled currents, we assume that the *direction* of the modeled currents is correct to a certain extent. We therefore select (Filter 2) only observations when $course_r$ falls within a given interval +/- of the modeled direction (in degrees).

Thus to remove as much "bad data" as possible, we have created the following three levels of filtering:

- Filter 0: Remove all data where SOG is less than 10 knots
- Filter 1: Remove all data where the absolute value of SOG-STW exceeds 2 m/s
- Filter 2: Remove all data where $course_r$ deviates more than (i) 5, (ii) 10, (iii) 20 and (iv) 30 degrees from the model current direction

2.3 Assessment of the ship data

We received data from the ship Samskip Kvitbjørn covering the period November 1, 2017 through April 5, 2020. The original ship data had a time resolution of 1 Hz, but since the ocean model Norkyst800 has a spatial resolution of 800 meters and a temporal resolution of 1 hour, the ship data was down sampled by the data provider to better fit the resolution of the model. The total number of observations delivered was therefore 292 571. For each location of observations we extracted simulated currents from the model grid point closest in time and space using the nearest neighbor method. By applying Filter 0 we were left with 277 172 observations. By applying all the filters consecutively (Filters 0, 1 and 2) listed in Section 2.2 the results in terms of number of observations at different model depths was as shown by Table 1.

	$\pm$5deg	$\pm$10deg	$\pm$20deg	$\pm$30deg
0 m	19 586	38 496	69 554	92 296
3 m	19 778	38 826	70 205	93 293
10 m	20 244	38 748	72 064	95 405

Table 1: Number of concurrent currents observed and modelled left for comparison when applying Filters 0, 1 and 2 at different model depths.

As shown by Figure 2 we observe that the main distribution of the ship's course lies between 320 to 70 degrees and between 150 and 260 degrees, with peaks close to 40 and 220 degrees. This is as expected since the Norwegian coast by and large has a north-south orientation and the ship mainly sails with goods along the coast. Also shown, and somewhat unexpected, is that the distribution of the relative current SOG-STW has a clear bias toward negative values with a median values of -0.04 m/s. Negative values of SOG-STW implies that the ship is sailing *against* the current. Thus Figure 2 indicates that the ship is spending more time sailing *against* the currents than *with* the currents. Whether this bias in the dataset is true or due to observational errors has not been assessed by us since it lies outside of the scope of this work and our area of expertise. In all further analyses the SOG-STW is handled as being "without errors". We emphasize, however, that this adds to the uncertainty of the observations. As mentioned, and as explained in Section 2.1, we need to do a conversion from the ship relative currents into some type of "absolute entity". After conversion the ship data have a distribution as shown by Figure 3.

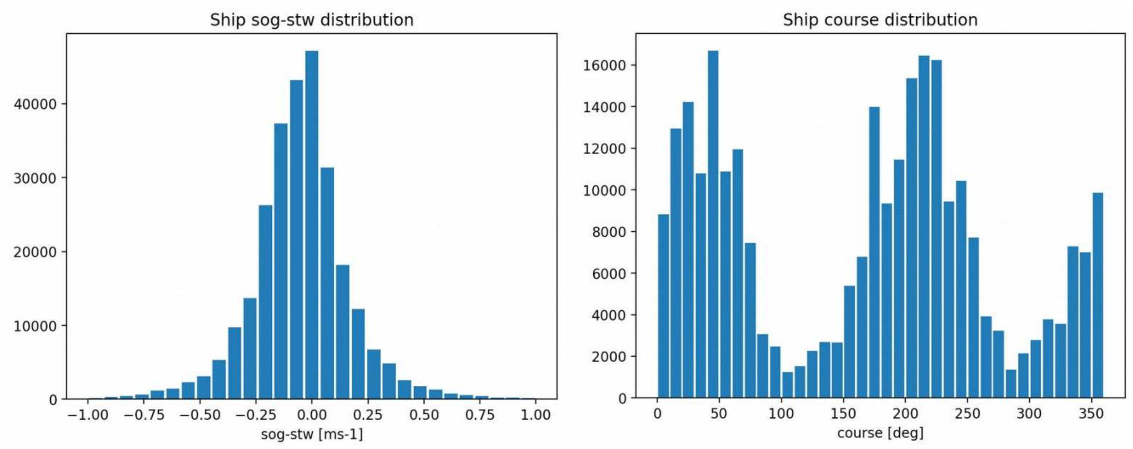

Figure 2: Frequency distribution of the relative current SOG-STW (left panel) and the ship's course (right panel) after application of Filter 0.

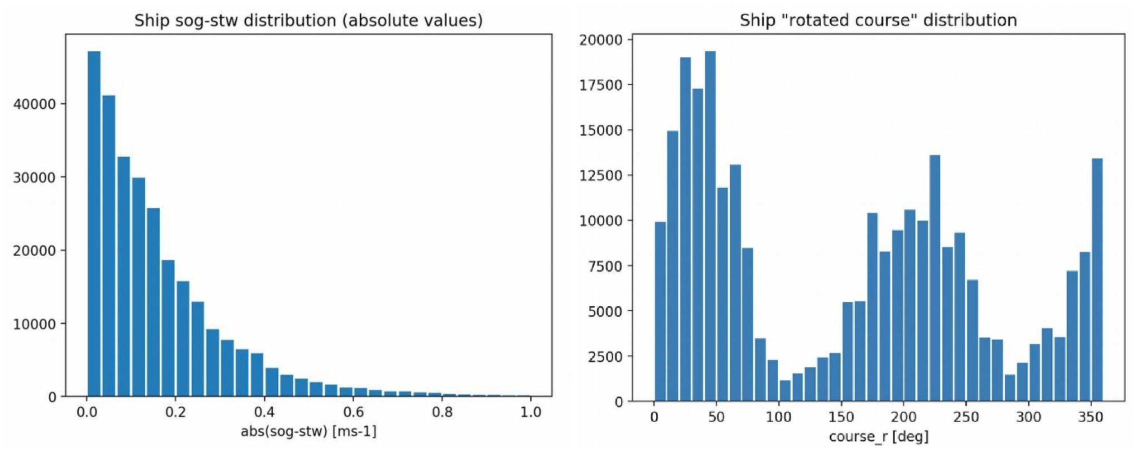

Figure 3: Similar to Figure 2, but showing the frequency distribution of the absolute values of the relative current (SOG-STW) and the relative direction ($course_r$).

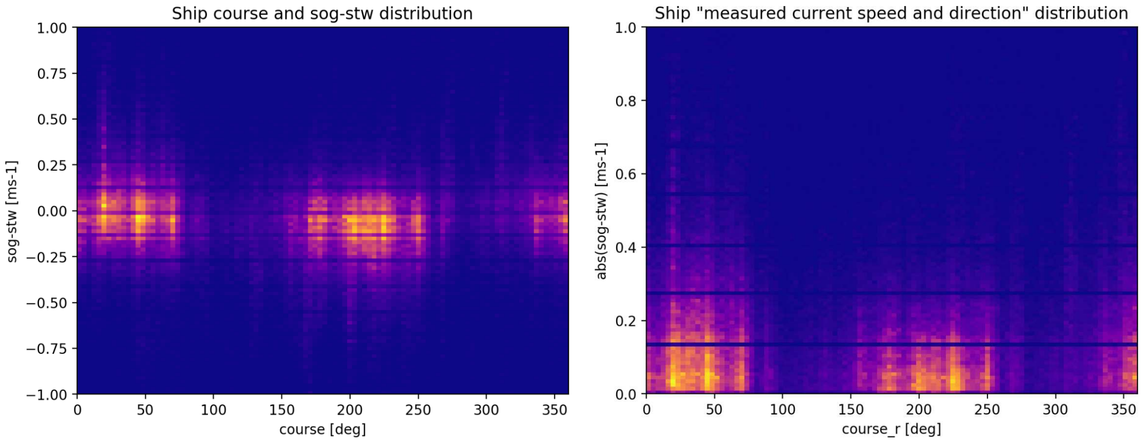

Figure 4: Heat maps showing the statistical distribution of the ship course and SOG-STW (relative current) data. Left-hand panel shows the data before conversion to absolute enteties, while the right-hand panel shows the data after conversion. Warmer colours indicate higher frequencies. Numbers along the horizontal axis are course in degrees, while the numbers along the vertical axis indicate speed in m/s. The “horizontal lines” that can be seen in the data is an artefact due to the conversion from knots to m/s and too low numerical precision of the original data.

The information presented by Figures 2 and 3 may be combined into so called heat maps as shown by Figure 4. The left-hand panel show how the main distribution of sailing with the currents occurs when the ship is sailing northwards, and how the main distribution of sailing against the currents occurs when the ship is sailing southwards. The right-hand panel shows the statistical distribution of the $course_r$ or the relative direction (along the horizontal axis) and the absolute values of SOG-STW (along the vertical axis). Warmer colors indicate higher frequencies. When we take into account that the main currents along the Norwegian coast is flowing northwards along the western coast of Norway this explains the patterns seen in Figure 4.

2.4 Acoustic Doppler Current Profiler (ADCP) data

As alluded to in the introduction (Section 1) we also have access to measurements from six moorings containing ADCP data located in a limited area off the northwestern coast of Norway referred to as the Sulafjorden area, a fjord system consisting of Breisundet, Sulafjorden and Vartdalsfjorden (Figure 5). For each location ADCP, CTD and Aquadopp (at 1 m) measurements are available. However, for our purpose we focus on the ADCP measurements available from 5 meters down to 25 meters. While mooring D is located in Breisundet at the far end of the fjord system towards the open sea, mooring F is located in Vartdalsfjoden well inside the fjord system and far away from the other moorings. Moorings A, B, B1, and C1 are located in the sound into Sulafjorden and Vartdalsfjorden. This gives us observations from four moorings in a rather limited area. While mooring A is deployed at the outer end of the sound, the three moorings B, B1 and C1 are located inside of A and across the fjord so that B is in the middle of the fjord, B1 at the eastern side and C1 at the western side. As indicated by Figure 5 there are only five grid points or less across the fjord where the latter ADCP instruments are moored. Keep in mind that this is probably not enough to realistically describe the fjord dynamics in any detail. For instance where the fjord system has its minimum width there is only two grid points across.

Although some of the E39 moorings were deployed already in 2016 (moorings A,B and D) the ship data are available only from November 2017 up to and including April 2020. Thus we have extracted ADCP data from the moorings for the time periods displayed by Table 3 only. Note that moorings B1, C1 and F were deployed in February 2019. The time resolution of the ADCP measurements are 1 minute. The quality of the measurements are relatively good, but the data have been run through a quality check,

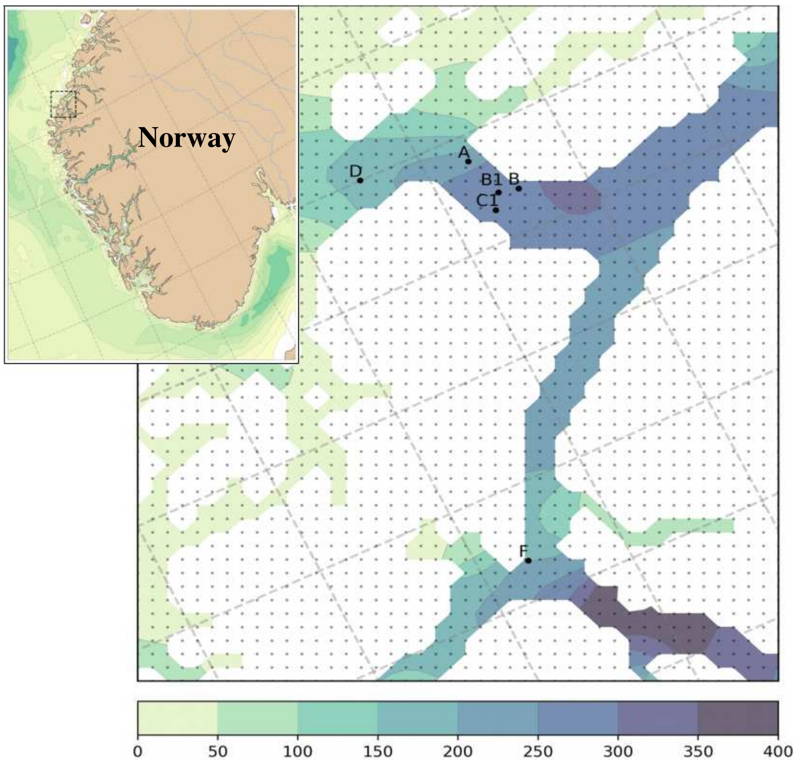

Figure 5: Distribution of moorings in Sulafjorden (A, B, B1, C1), Breisundet (D) and Vartdalsfjorden (F) as part of the project “Fergefri E39” at the West Coast of Norway. The color scale ranging from 0 to 400 meters indicates the depth of the NorKyst800 model in the area. Also shown are the grid points of the model (small gray dots).

where the outliers have been removed. To cancel some of the noise, the data were first filtered with a 10 minutes running mean before it were down sampled to a 1 hour data set to better fit the temporal resolution of the NorKyst800 model. ADCP current measurements are available for every 5 meters depth level, but for this work we have only validated the currents at 5, 10, and 25 meters. The corresponding depths from NorKyst800 are 3, 10 and 25 meters. Note that we compare the observations from 5 meters depth with the model output from 3 meters depth. The background for this is that we want to use model data that is publicly available, even though it will probably result in a bias in the comparison since the model is more slightly energetic at 3 meters depth compared to at 5 meters.

3 Assessment of NorKyst800 against ship data

We have extracted corresponding ocean model predictions of current speed and direction from the nearest grid point and time step to compare with the observational ship data set. The model offers multiple choices of vertical levels of currents, and we have selected the depth of 0, 3 and 10 meters in this comparison. The unfiltered data is shown by Figures 6, 7 and 8. As can be seen in the figures, the statistical distribution of current direction is very similar between the different vertical levels, but the distribution of current speed varies more. It is clear that from the vertical levels we have chosen, the most comparable distribution of current speed between the model and the observations is found at 10 meters depth (Figure 8). All three figures also show that for direction, there is a large amount of the data where there is no overlap between observations and model. This explains why large amounts of the data is filtered out when applying our filters described in Section 2.3.

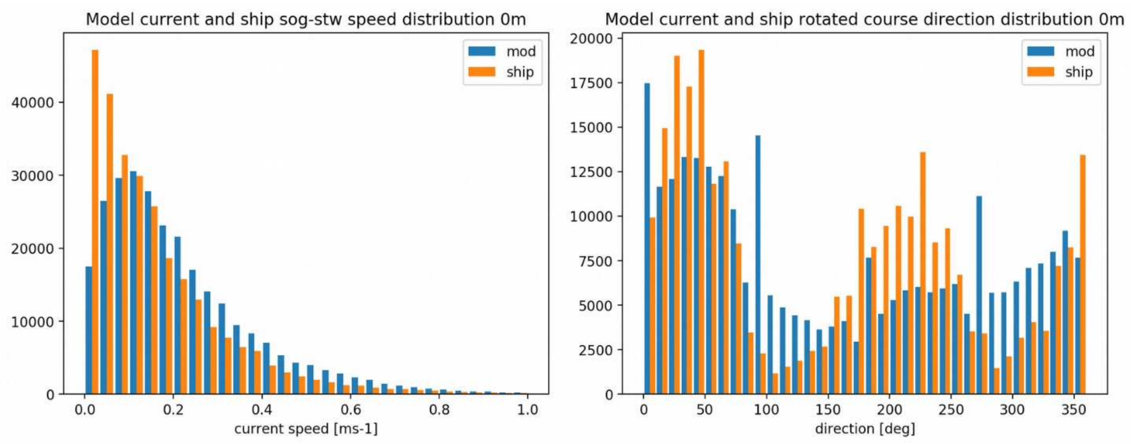

Figure 6: Statistical distribution of model current speed (left panel) and model current direction (right panel) at 0 meters depth at the times and positions of the ship data. Ship data are also shown.

In the remaining part of this assessment we apply all the filters (Filters 0, 1 and 2) as described in Section 2.2 using all the model output from the three different depth levels. Model output are corrected to only reflect the current speed component[1] that is in the same direction as the rotated course from the ship. The comparisons as shown in Figure 9, 10 and 11 show that the model and the observations differ quite a lot when comparing

[1]Corrected_current_speed = current_speed*cos(current_direction - $course_r$)

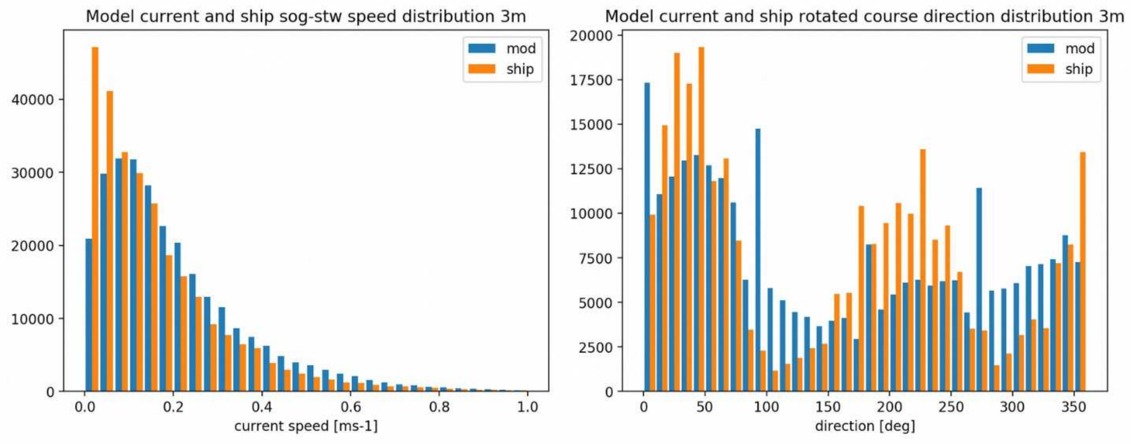

Figure 7: Same as Figure 6, but for 3 meters depth

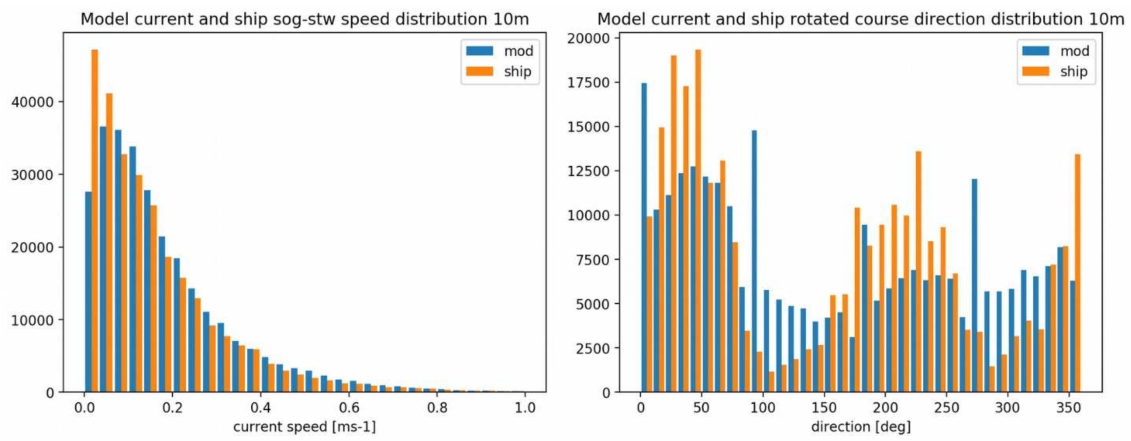

Figure 8: Same as Figure 6, but for 10 meters depth

current speed at the same time and place (green dots), but has a better agreement when the data is sorted according to value magnitude. This tells us that, given that the SOG-STW could be used as a proxy for the current and that the actual current experienced by the ship is the same as the current direction from the model, the model has a very realistic statistical distribution of current speed, whereas the forecast skill is less good. Correlation coefficients between modeled and observed current speed is shown in Table 2. The highest correlation is found when comparing observations against modeled currents from 10 meters depth. We therefore chose to use only model output from 10 meters in the rest of this comparison, since we believe this is the depth that that best reflects the current that affects the ship Samskip Kvitbjørn.

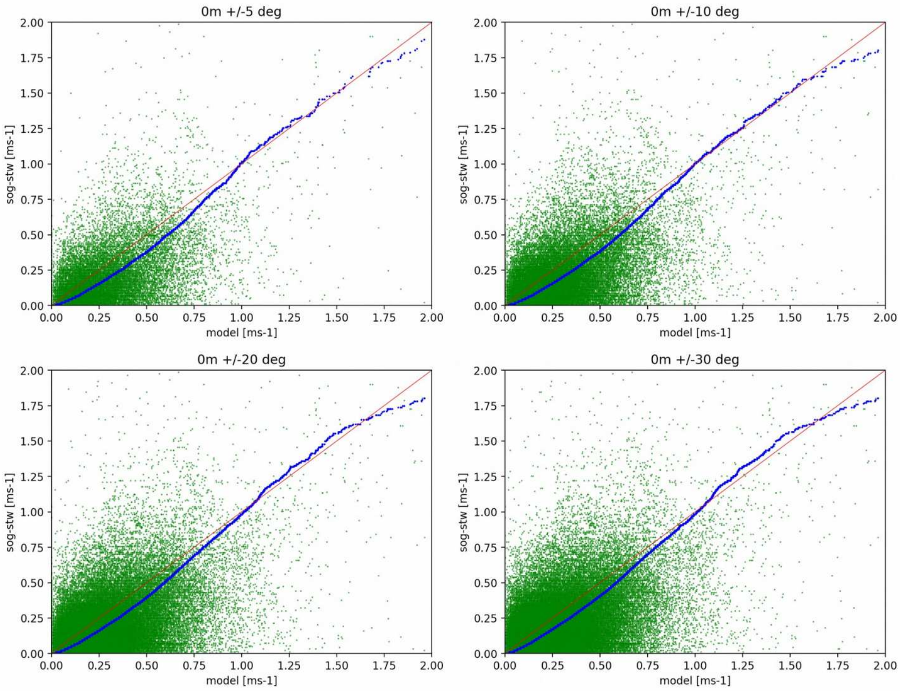

Figure 9: Comparison of modelled and observed current speed at 0 meters depth after applying all Filters listed in Section 2.1. The green dots compose a scatter diagram comparing each observation and model at the same time an position, whereas the blue dots represent a so called qq-plot in which the data are sorted in ascending order of current speed to illustrate the statistical distribution of the model versus observations. The axis has been limited to 2 m/s since the major part of data falls within this range. The red diagonal line represents the 1-1 line where a perfect fit between model and observations would be located.

Correlation	**±5deg**	**±10deg**	**±20deg**	**±30deg**
0 m	0.479	0.480	0.472	0.465
3 m	0.502	0.493	0.482	0.476
10 m	0.521	0.516	0.509	0.504

Table 2: Correlation coefficients for the scatterplots (green dots) shown by Figures 9, 10 and 11.

Figures 11 and 12 show that the majority of data from both observations and model has a current speed magnitude less than 0.5 m/s. It is also quite clear that there is a tendency for the model to overestimate the weaker currents, whereas it tends to underestimate some of the stronger currents. As mentioned earlier, the method used in this comparison has big uncertainties, so trying to give a precise explanation of the over-/underestimation from

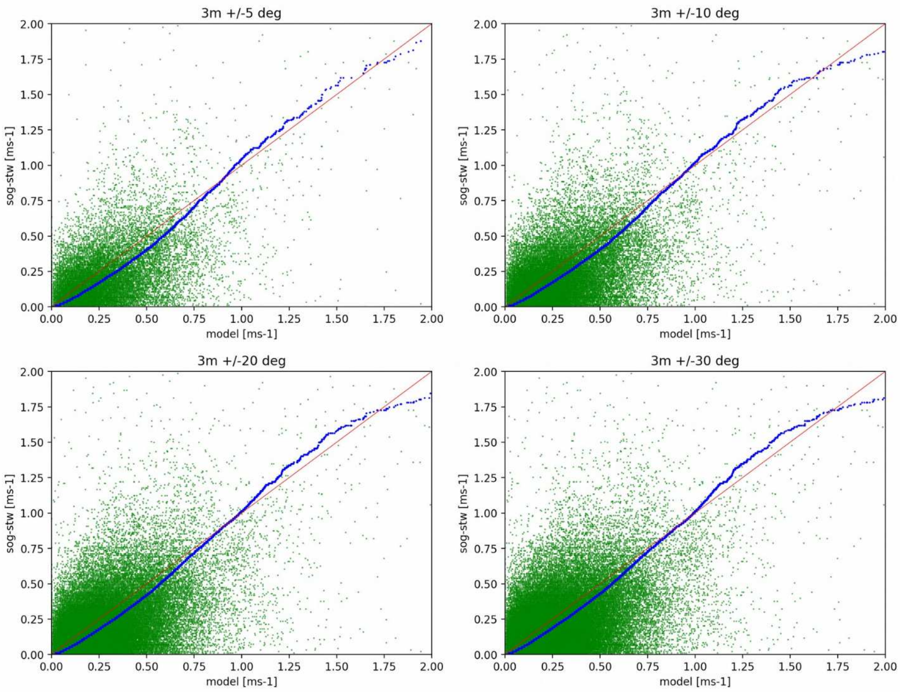

Figure 10: Same as Figure 9, but for 3 meter depth.

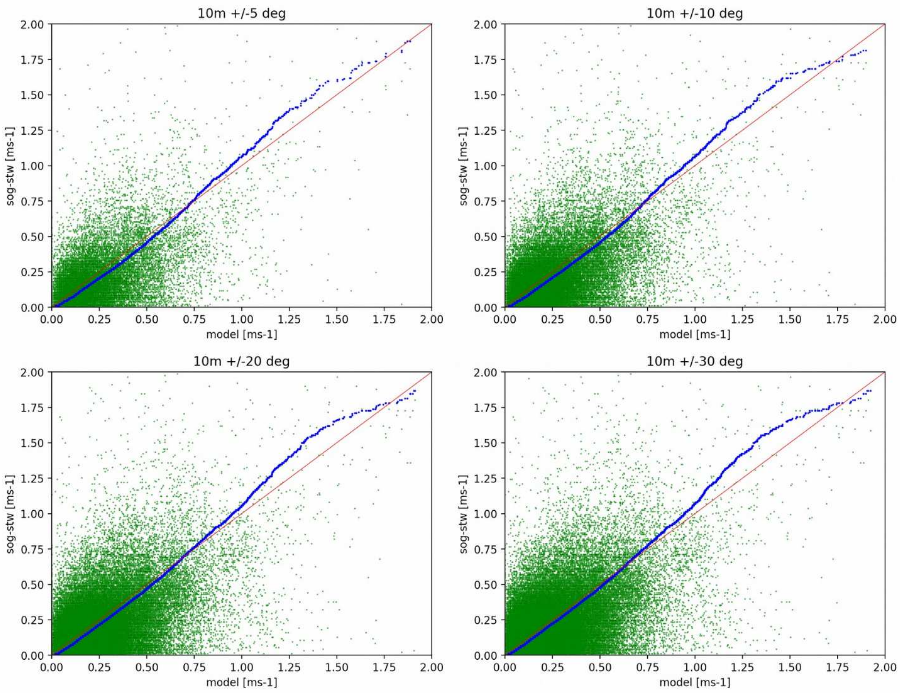

Figure 11: Same as Figure 9, but for 10 meter depth.

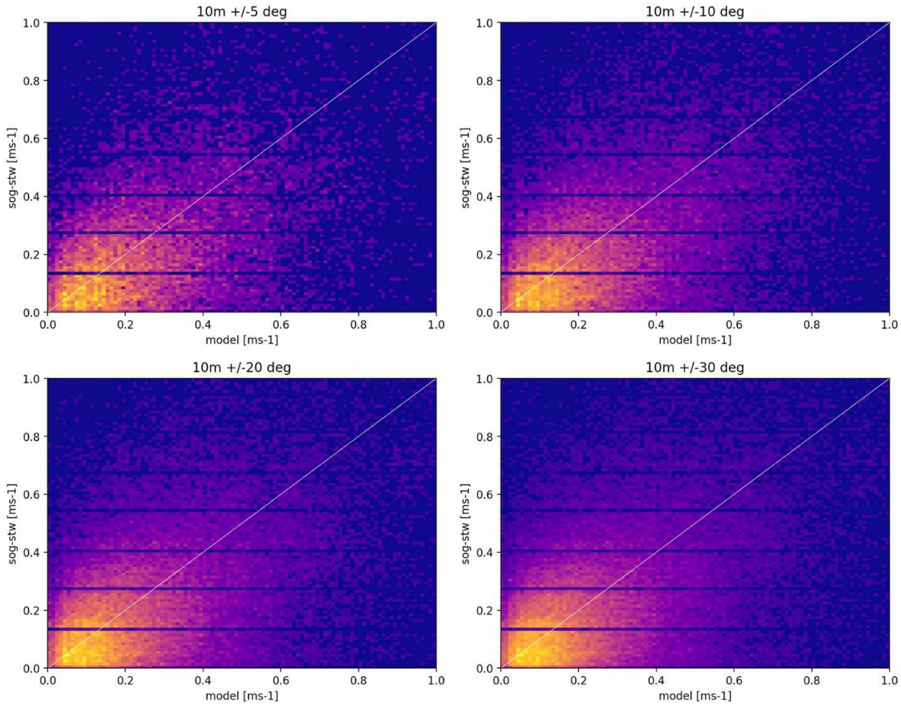

Figure 12: Same as Figure 11 (green dots), but showing data as heat maps to better visualize the data distribution.

the model is difficult. However we would like to again point out the fact that due to how the currents are observed in this study, the SOG-STW that we use as a proxy for current speed, is likely to always be less than the actual current speed. In fact, unless the actual current flows in the exact same direction (or opposite) as the ship course, the value of SOG-STW is less than the real current speed. This could probably explain why the model seems to have a tendency to overestimate the current speed in the range of 0 – 0.5 m/s, which is also the range where most of the data is found (see also Figure 13). The models tendency to underestimate the larger values of current speed (> 1 m/s) we believe is due to the somewhat limited model resolution, when taking into account that the ship sails along a coast with narrow straits and fjords with size in the same order of magnitude as the model.

It is interesting to note that although the correlation between the model current predictions and observations are highest when applying the strongest criterion for Filter 2 (a maximum difference between model current direction and rotated ship direction of ± 5 degrees), it seems like the similarities in statistical distribution of model output and data increase when the criterion for direction difference is "relaxed". We currently do not

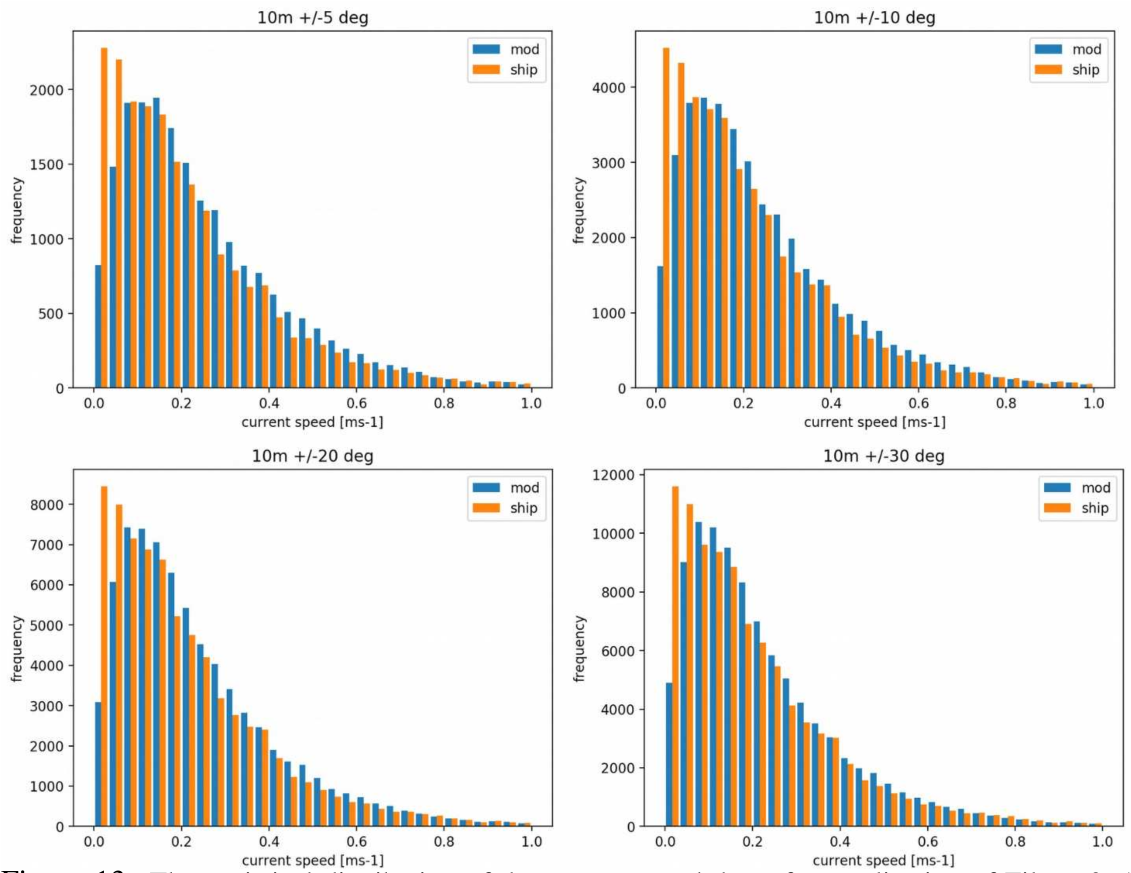

Figure 13: The statistical distribution of the current speed data after application of Filters 0, 1 and 2 for different intervals of difference between model current direction at 10 meters depth and ship rotated course.

have a good explanation for this, other than to speculate that it could be an effect of the increased number of data points with a factor close to 5 (cf. Table 1).

Figures 14 and 15 show the geographical distribution and location of the data used in this study. Figure 14 show the difference between the model and the observations scaled by the standard deviation of the observations. In Figure 16 we show the difference between current direction and ship rotated course. The data has been limited to where the difference is less than 30 degrees. At first glance it may seem like there are many areas where the difference between model and “observation” is high. That is correct, however, we must emphasize that this does not mean that the model is wrong! It is simply a measurement of how much deviation there is between the ship rotated course and the model current direction. So instead of interpreting Figure 16 as a figure that says something about model quality, we urge the reader instead to interpret it as a figure that show where we expect the highest quality and number of data points used in the comparison is found. Detailed maps can be found in the appendix on page 47.

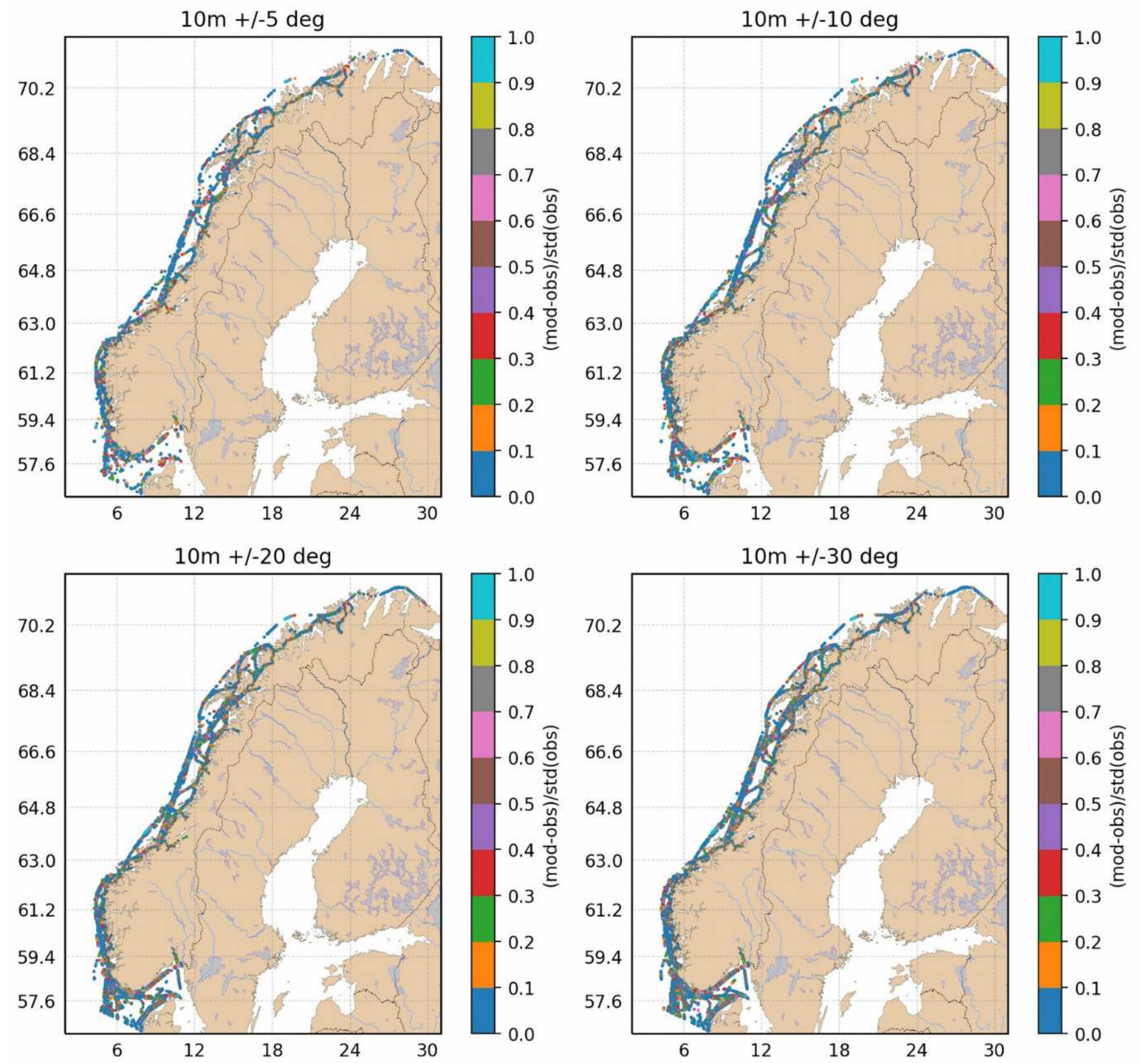

Figure 14: Maps showing the difference in model current speed at 10 meters depth and ship SOG-STW scaled by the standard deviation of SOG-STW (approximately 0.4 m/s). The maps also give an impression of the geographical distribution of the data given the different criterion for difference between model current direction and ship course in Filter 2.

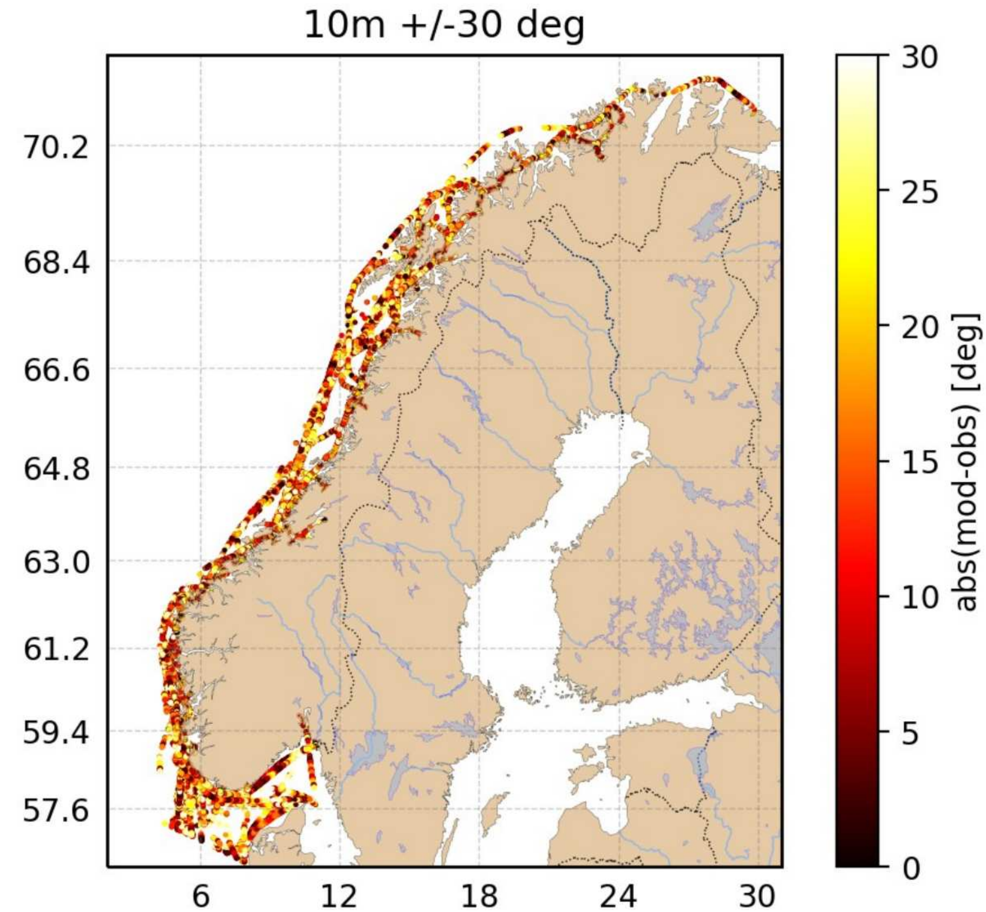

Figure 15: Map showing the absolute difference between model current direction at 10 meters depth and ship rotated course, allowing for differences up to +/- 30 degrees. Note that a big difference here does not translate into a large model error in direction. It simply shows that the ship course is not parallel to the current direction. Warm (dark) colours indicate that the ship course is close to parallel with the current direction.

4 Focused comparisons in the area of Sulafjorden

4.1 Comparison of observed ADCP currents and model output

We have extracted corresponding ocean model predictions of current speed and direction from the nearest grid point and time step to compare with the data made available to us from the ADCPs in the Sulafjorden area. Table 3 below gives an overview of the time period and depths used in the comparison data for each mooring.

Station	Time	Depth ADCP [m]	Depth NorKyst800 [m]
Sulafjorden: A,B	2017.11 – 2020.04	$5, 10, 25$	$3, 10, 25$
Sulafjorden: B1,C1	2019.02 – 2020.04	$5, 10, 25$	$3, 10, 25$
Breisundet: D	2017.11 – 2020.04	$5, 10, 25$	$3, 10, 25$
Vartdalsfjorden: F	2019.02 – 2020.04	$5, 10, 25$	$3, 10, 25$

Table 3: An overview of ADCP measurements available for each mooring. Notice that moorings B1, C1 and F have a shorter time series of data than A, B and D, and when we evaluate currents at 3 meters depth in NorKyst800, the corresponding depth in the observations is at 5 meters.

4.1.1 Breisundet (station D)

Figures 16 and 21 show the validation results for station D, which is located at the outer end of Breisundet. Here the model has some more grid points across the fjord than further into Sulafjorden. We see that the observed water transport mainly flows in and out of the fjord, in a westerly and easterly direction and that the model has the same pattern. This especially applies to the upper depths (5 and 10 meters). At 25 meters, both the model and the observations have a more easterly current direction into the fjord. The variability of the currents are well described by the model in this area, but as Figure 19 illustrates the model speed is underestimated for all depths except at 5 meters, but for this depth the model results represent the speed at 3 meters which may be the reason for the higher speed in the model relative to the observations at this depth.

4.1.2 Sulafjorden (stations A, B, B1 and C1)

Station A is located in the outer part of Sulafjorden and the flow is mainly northerly and southerly along the fjord as illustrated in Figure 17. Between 5 and 10 meters, the currents

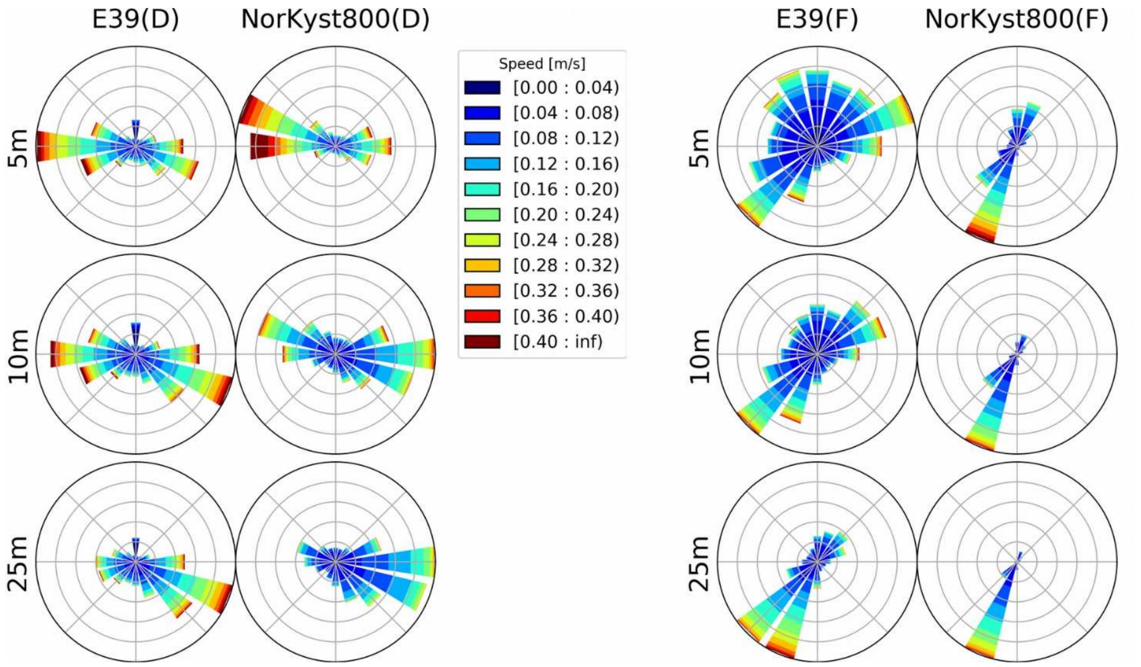

Figure 16: Current rose plots of current speed and direction at station D in Breisundet (left panel) and at station F in Vartdalsfjorden (right panel). The locations of the stations are as displayed by Figure 5. Left column of each panel represent data from the ADCP at 5 meters, 10 meters and 25 meters depth for the time period specified in Table 32. Right column shows the corresponding model results, except that the upper model rose plot is at 3 meters.

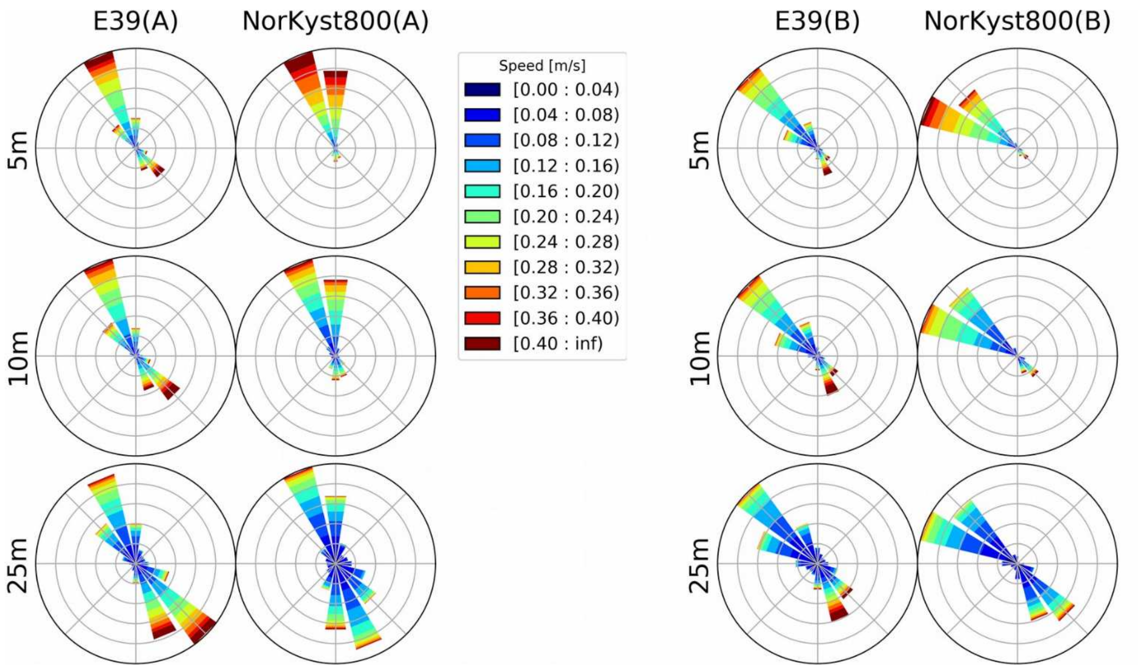

Figure 17: Same as Figure 16, but for station A (left panel) and C1 (right panel).

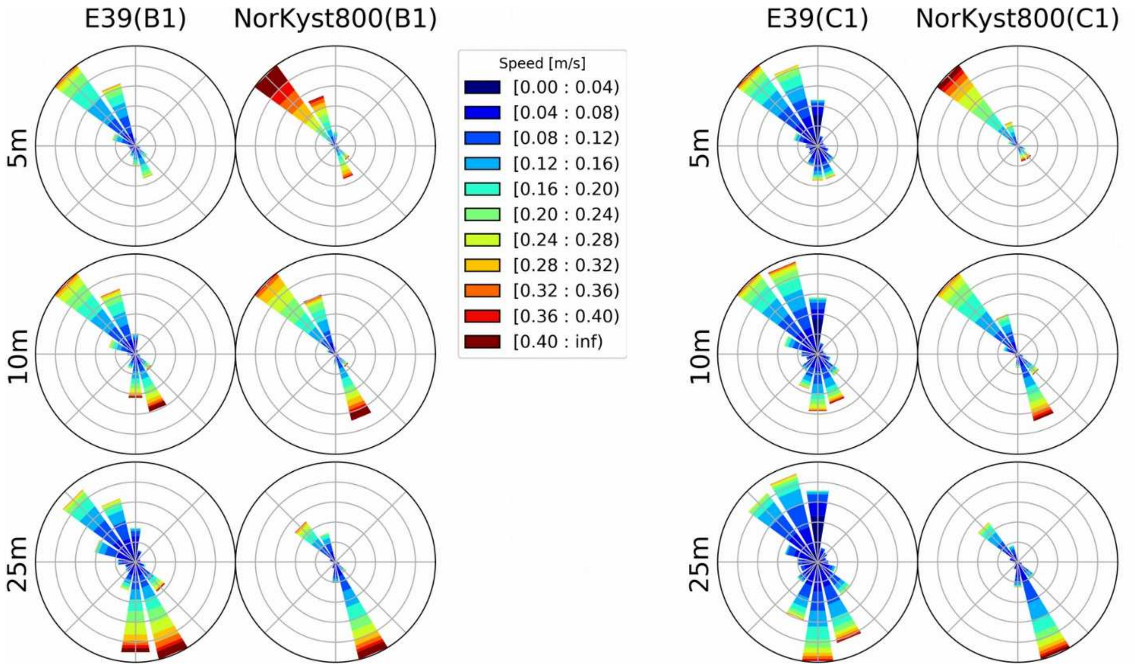

Figure 18: Same as Figure 16, but for station B1 (left panel) and C1 (right panel).

are mainly outgoing in a northerly direction. We see the same pattern in the model as in the observations. Also the variability in the current field is well described by the model, even though the resolution of the model is only 800 meters. Here, too, the current speed is underestimated in the model, except in the upper depth (where observed current speed at 5 meters is compared against modeled speed at 3 meter), as shown in Figure 19.

Station B and B1 are located in the eastern part of Sulafjorden south of station A, and the main flow in this area is northwesterly and southeasterly. For this part of the fjord there is a good agreement between the modeled current speed and the observed current speed, as shown by Figure 20 and 21. Also the variability seen in the current field is well represented in the model as illustrated by Figure 17 and 18. Station B covers the period November 2017 to April 2020, while buoy B1 was not installed before February 2019.

Station C1 is situated in the western part of Sulafjorden and there is a good agreement between the distribution of the modeled and the observed current speed (Figure 21), however the model is not able to reproduce the variability observed in the current field in this part of the fjord as illustrated by Figure 18.

4.1.3 Vartdalsfjorden (station F)

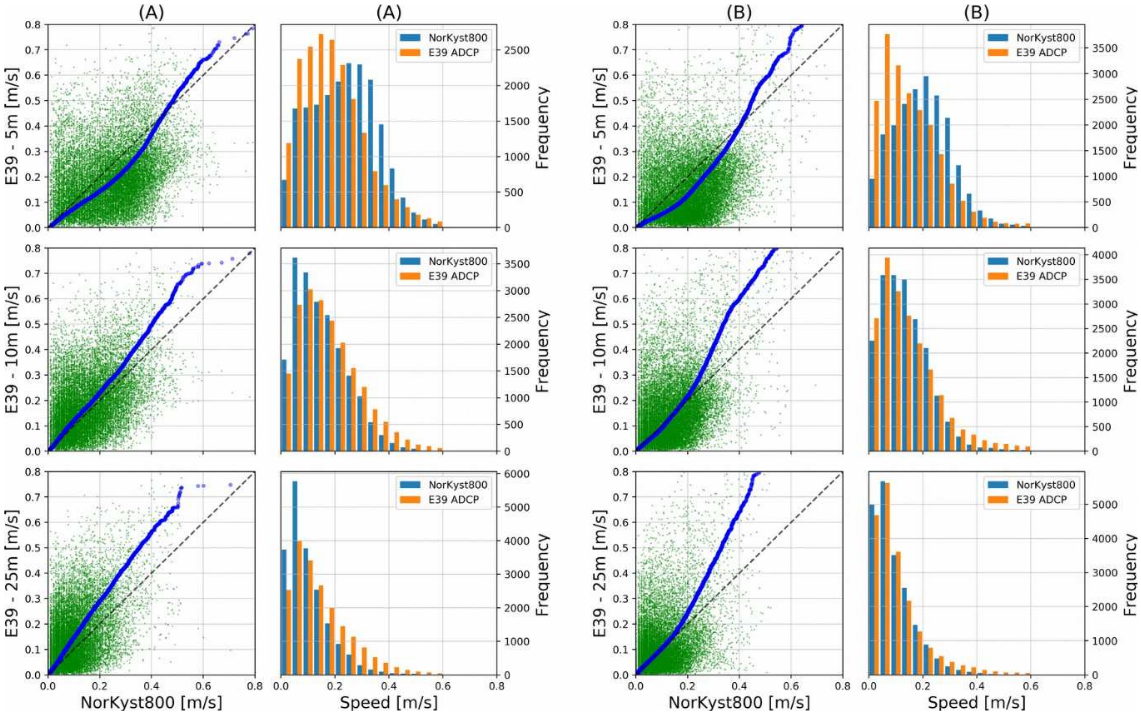

Figure 19: Comparison of current speed from model and ADCP at station A (left) and B (right). Top row is 5 meters, second is 10 meters and bottom is 25 meters depth. Left-hand column for each station shows scatterplots (green dots) combined with qq-plots (blue dots) with model output along the horizontal axis and observations from ADCP along the vertical axis. The right-hand column for each station are the histograms or frequency plots of current speed distributions from the model and observations.

At station F, even with a inaccurate description of the bottom depth and limited grid points across the fjord, the model achieves a realistic distribution of current speed, as shown by Figure 16 and 22. However, the speed is somewhat underestimated. As illustrated by the current rose in Figure 16, the model is able to describe the main current direction to the south west, but is not able to represent the observed variability. In addition to an inaccurate bottom depth, the coarse resolution will also give an inaccurate description of the coastline. Narrow straits, that may be important for the fjord dynamics, will in some cases be closed. In addition, as shown in Figure 5, Station F is almost located on land in the model, while this is not the case in reality.

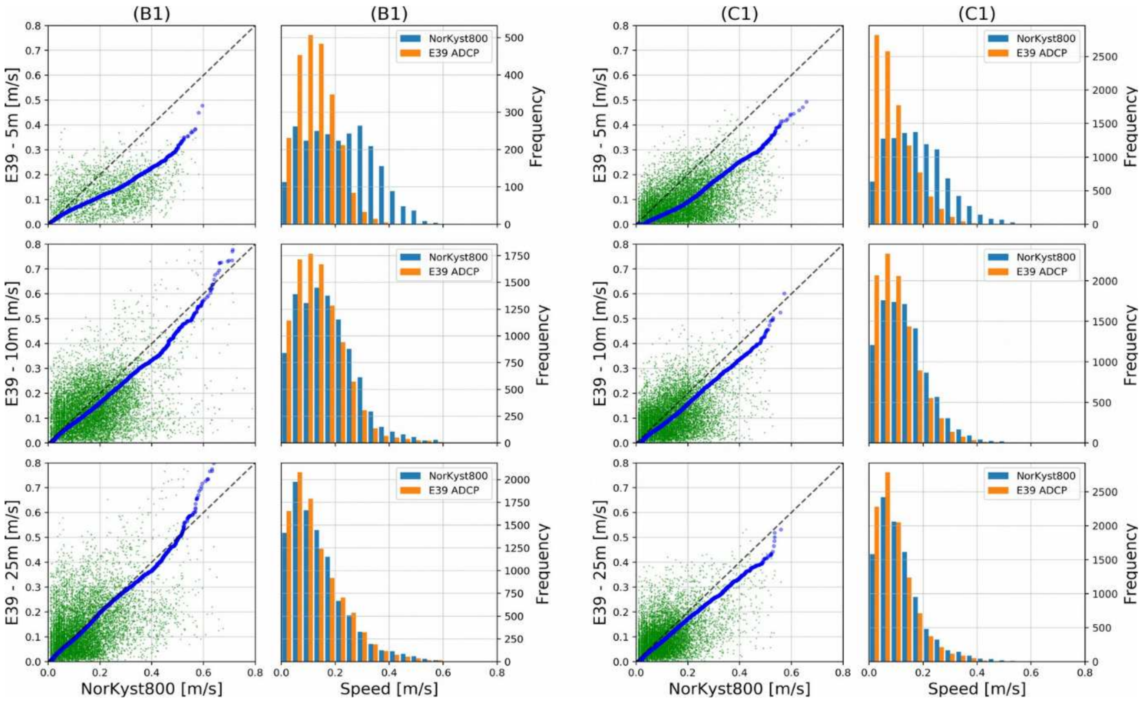

Figure 20: Same as Figure 19, but for station B1 and C1.

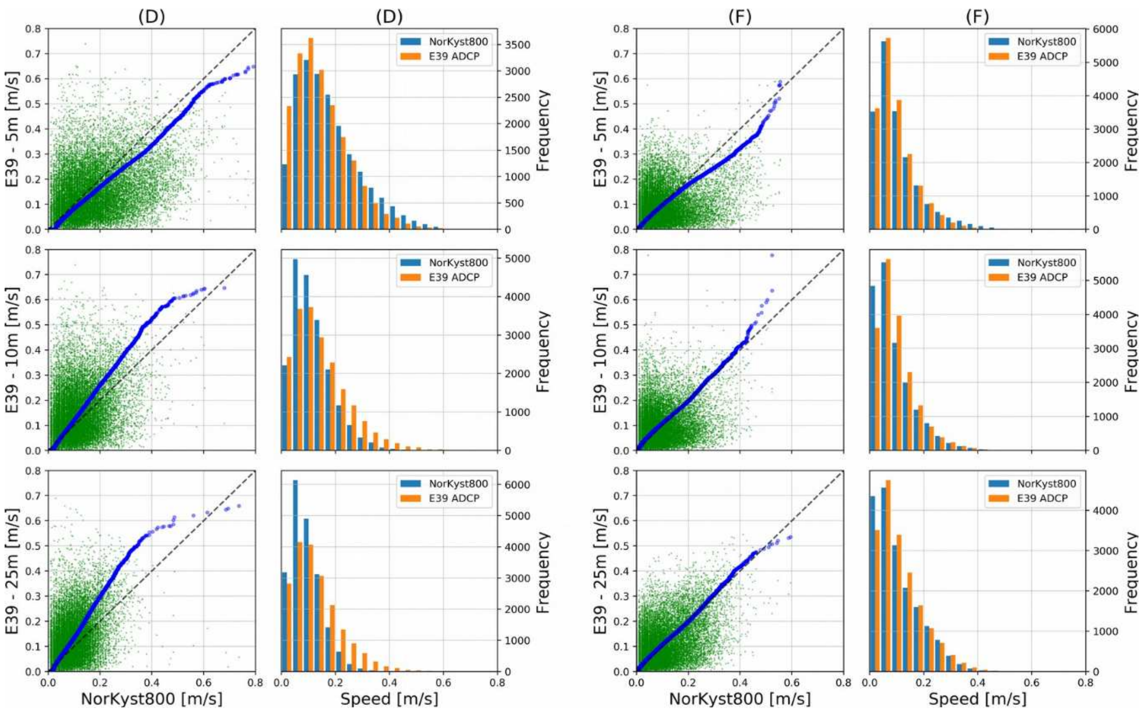

Figure 21: Same as Figure 19, but for station D and F.

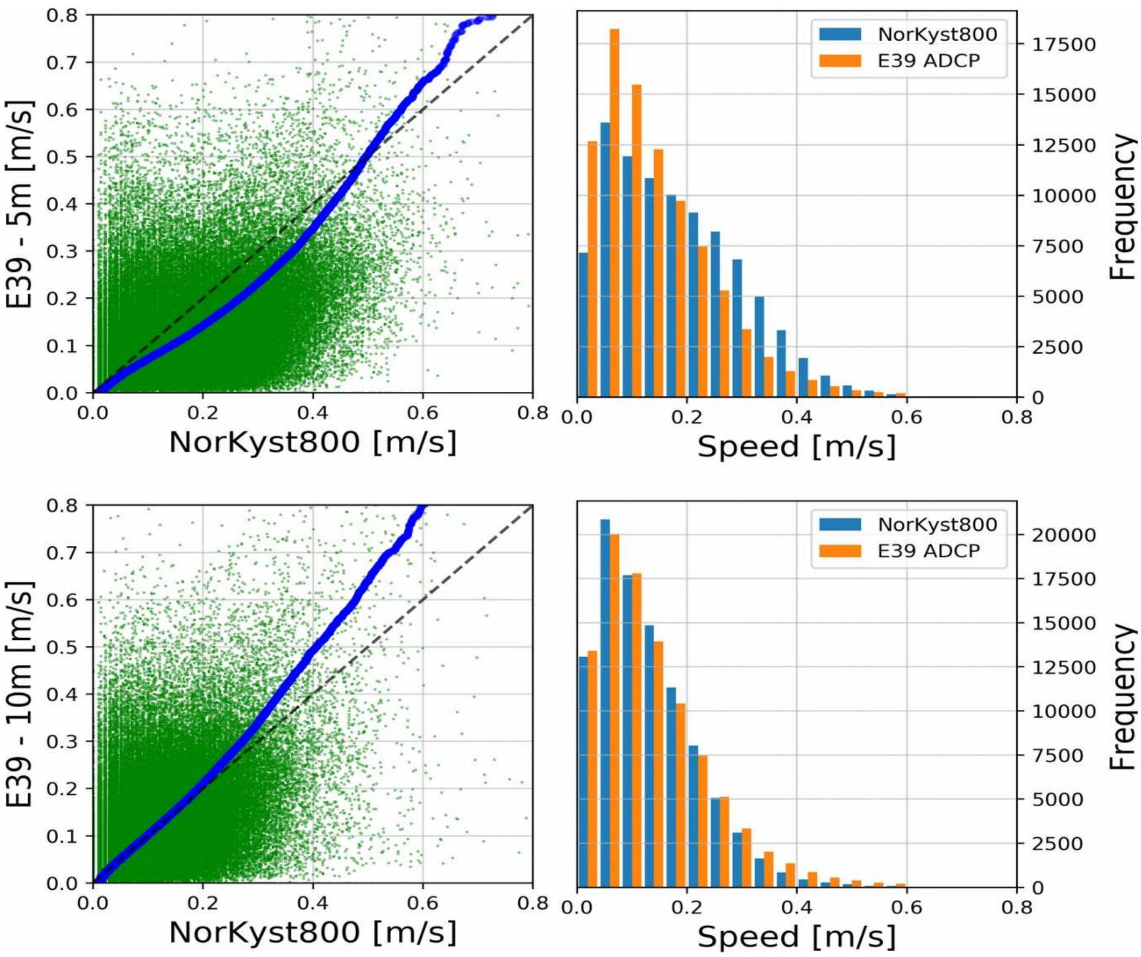

Figure 22: All stations from Figures 19 trough 21 combined and plotted in one single plot at 5 (top row) and at 10 meters depth (bottom row).

4.2 Ship data and model output comparison

To evaluate our method of comparing ship SOG-STW data with modeled currents, we have defined a sub-area of the data presented in Section 4 that corresponds to the area shown by Figure 5 studied in Section 4.1. The geographical limits are chosen to be between 62.19 – 62.47 °N and 5.8 – 6.2 °E.

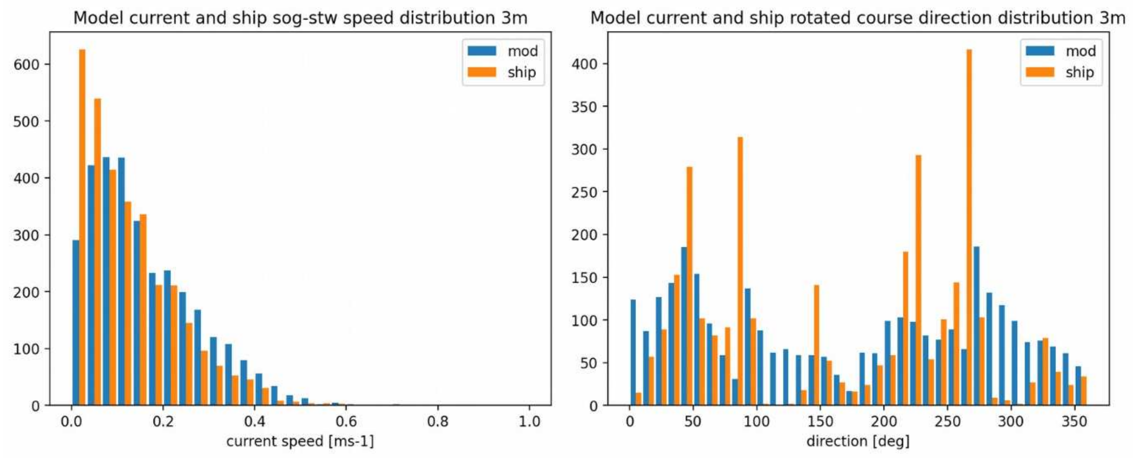

Figure 23: Statistical distribution of model current speed (left panel) and model current direction (right panel) at 3 meters depth at the times and positions of the ship data limited to the geographic area of Sulafjorden (62.19 – 62.4 N and 5.8 – 6.2 E). Corresponding ship data are also shown.

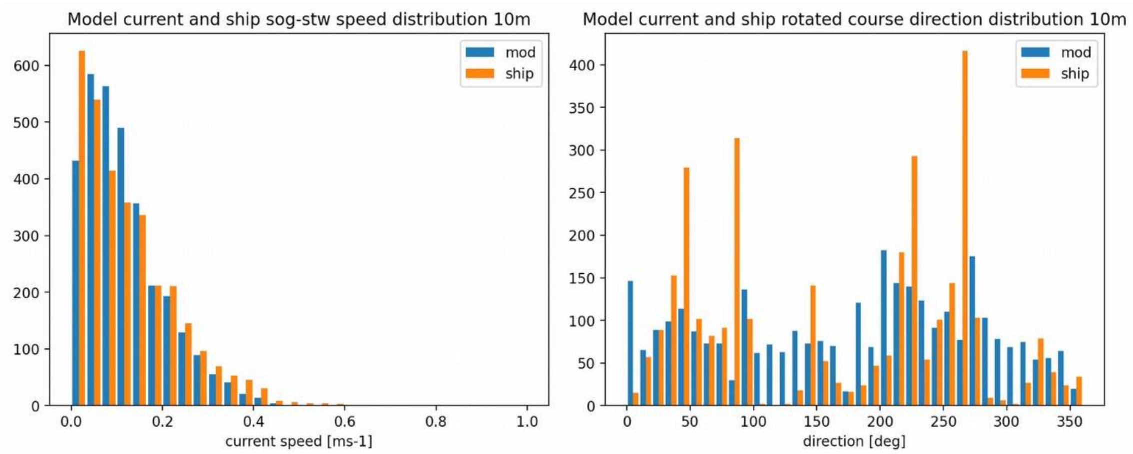

Figure 24: Same as Figure 23, but for 10 meters depth.

The statistical distribution of current speed from the model and ship measured SOG-STW is shown in Figures 23 and 24. As can be seen in the right panels in both figures, the ship rotated course direction has a few "peaks". This is a result from the fact that the ship (obviously) has to follow the path and direction of the narrow fjord, whereas we clearly see that the model output has a more evenly distributed directional distribution. However, one can argue that there are in fact a few "peaks" in the model output as well that correspond to the peaks in the ship rotated course ($course_r$).

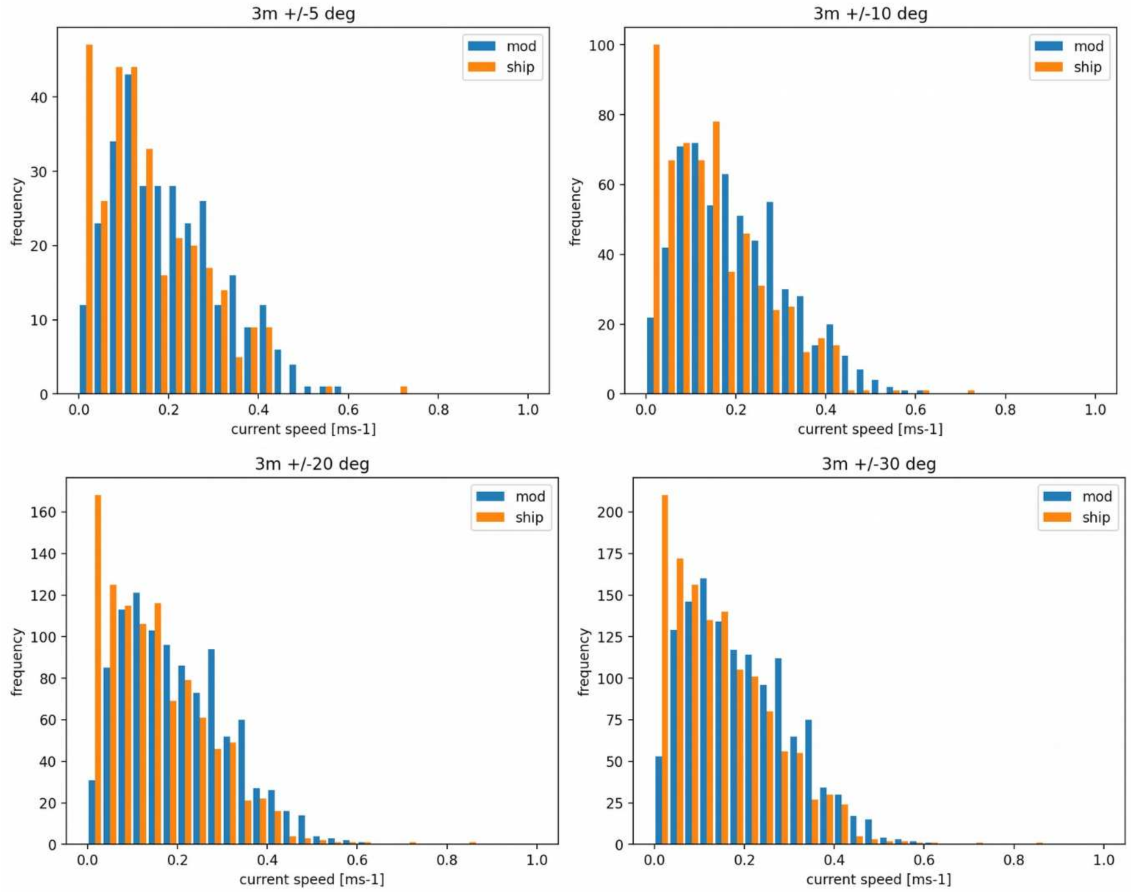

Figure 25: The statistical distribution of the current speed data after application of Filters 0, 1 and 2 for different intervals of difference between model current direction at 3 meters depth and ship rotated course limited to the geographic area of the Sulafjorden area (62.19 – 62.4 N and 5.8 – 6.2 E).

The geographical limitations decrease the number of data points in our comparison quite a lot, and the number of points available at each depth level after filtering and for each Filter 2 setting can be seen in Table 4. After applying the filtering algorithms as defined in Section 2.2 we get the results as shown in the following Figures 25, 26, 27 and 28.

The correlation between the model predictions and the observed currents from the ship

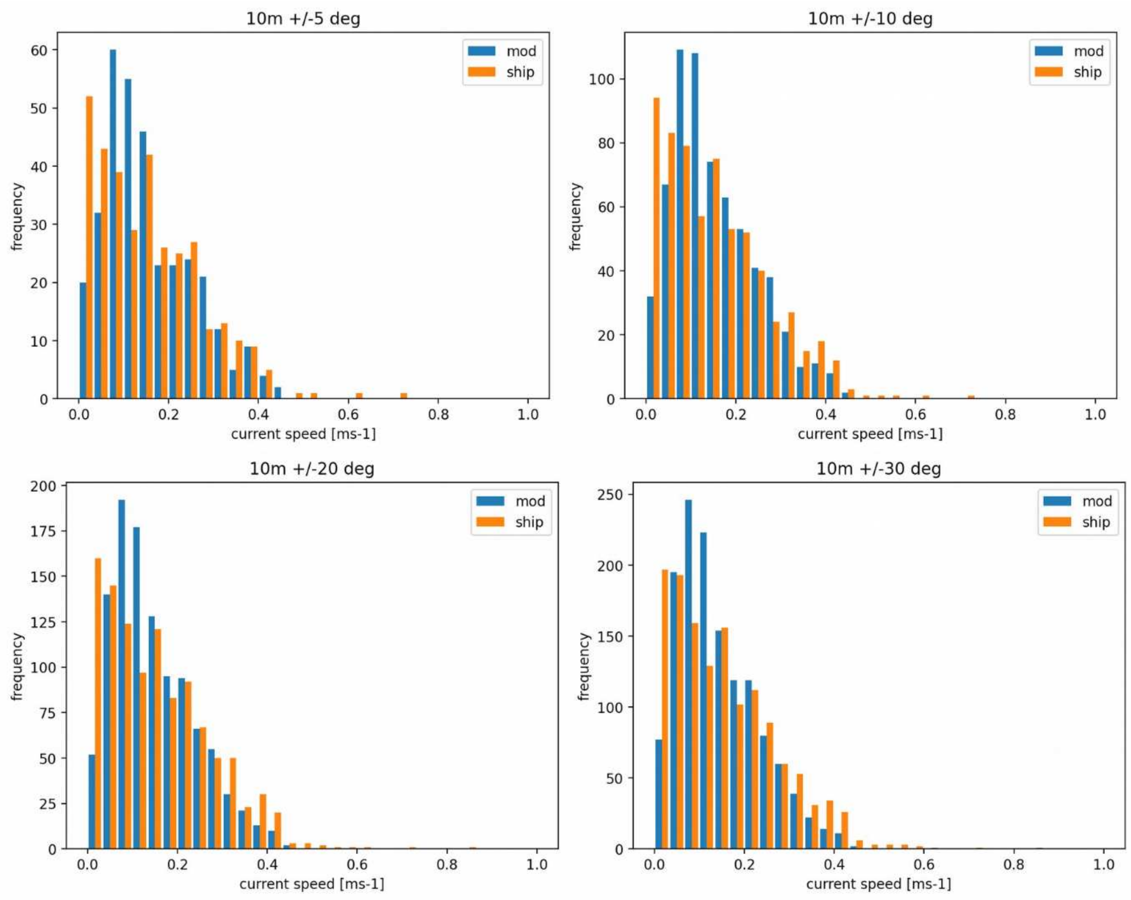

Figure 26: Same as Figure 25, but for 10 meters depth.

Depth	±5deg	±10deg	±20deg	±30deg
3 m	307	592	1007	1307
10 m	336	637	1075	1361

Table 4: Number of ship and model data points left for comparison for the limited geographic area of Sulafjorden after applying Filter 0, 1 and 2 for various intervals of differences between ship relative course and model current direction and for different depths of the modeled currents.

is weak as seen in Table 5. The statistical distribution of current speed however seems to be quite similar between the modeled and observed currents as can be seen by Figures 25 and 26, and Figures 27 and 28. The model has a tendency towards overestimating the weakest currents, and underestimate the strongest currents. There could be many reasons for this, but limited horizontal resolution in a narrow fjord is a prime suspect.

A more thorough study of the Breisundet and Sulafjorden area can be found in *Albretsen and Asplin* (2021).

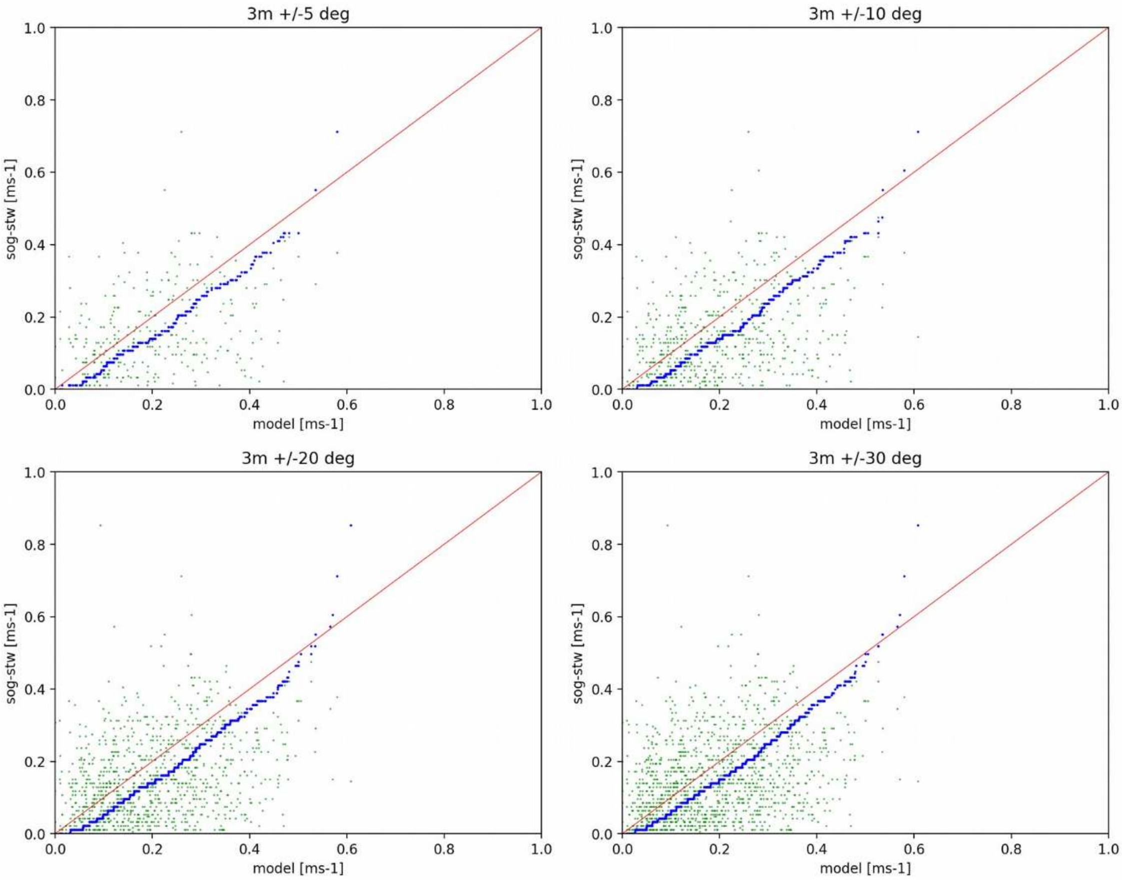

Figure 27: Comparison of modelled and observed current speed at 3 meters depth for four different maximum values of difference between model and ship rotated currents limited geographically to the Sulafjorden area (62.19 – 62.4 N and 5.8 – 6.2 E). The scatterplots are the green dots, while the blue dots are the qq-plots. Model output is along the horizontal axes and the observations are along the vertical axes. The red diagonal line represent the 1-1 line where a perfect fit between model and observations would be located.

Correlation	**±5deg**	**±10deg**	**±20deg**	**±30deg**
3 m	0.299	0.309	0.301	0.290
10 m	0.330	0.354	0.354	0.343

Table 5: Number of ship and model data points left for comparison for the limited geographic area of Sulafjorden after applying Filter 0, 1 and 2 for various intervals of differences between ship relative course and model current direction and for different depths of the modeled currents.

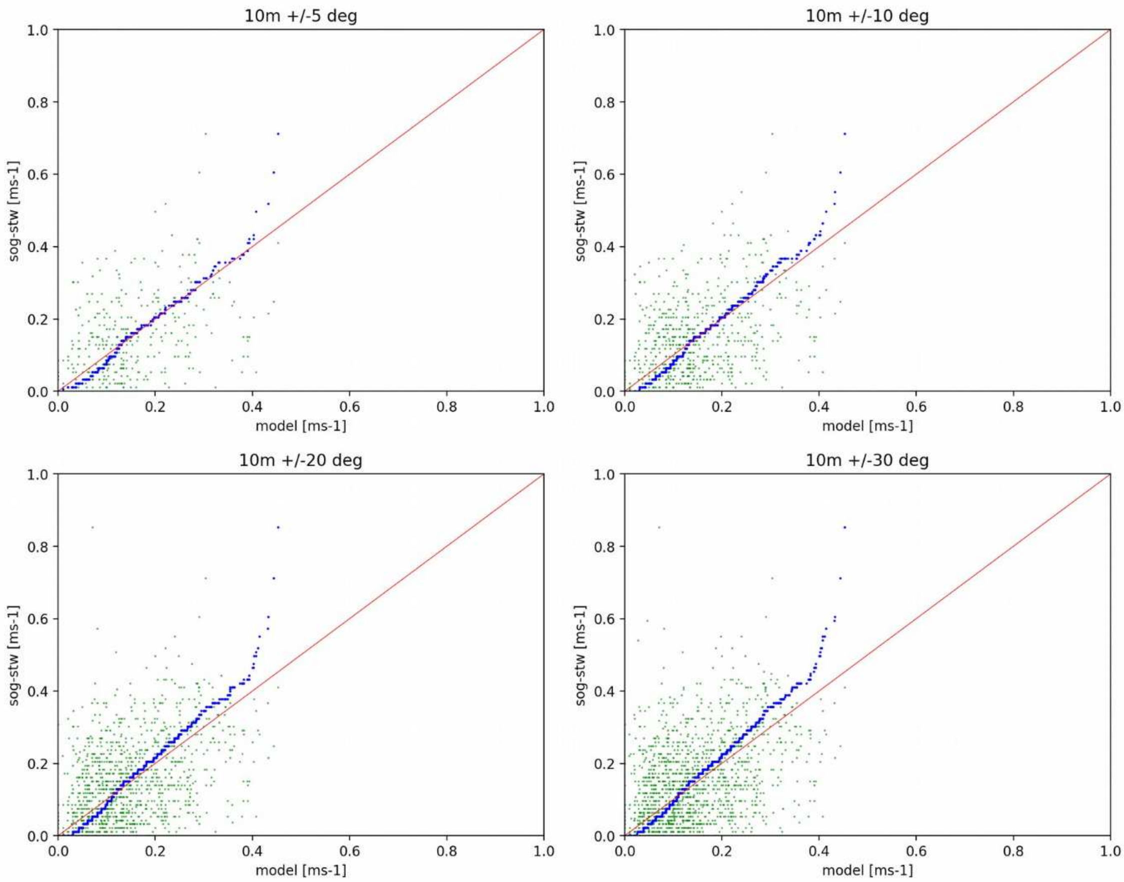

Figure 28: Same as Figure 27, but for 10 meters depth.

5 Discussion and remarks

Above (Section 4) we investigated whether the method developed in Section 2, in which primitive ship data like *speed through water* (STW), *speed over ground* (SOG), and *course over ground* (COG) and GPS position was converted into a proxy for the true current speed, was valid. We argue that the method presented is useful and may give valuable information about the performance and quality of current models. Nevertheless, we admit that more work are needed to quantify the uncertainties in the method of converting primitive ship data to true currents.

Given that the method appears to have some value we used it to convert primitive ship data from Samskip Kvitbjørn while it was sailing along the entire Norwegian coast. This provided us with a large data set of primitive ship data spanning approximately 2.5 years and covering a large part of the NorKyst800 model domain. We then used this converted observed currents to assess the quality of the modeled currents by the ocean model NorKyst800. When we compared the statistical distribution of current speed from the model with the converted observations from the ship, e.g., Figure 13, we noticed that they were very similar except at very low current speeds. We take this to imply that the observed and modeled currents have similar climatology and hence are comparable. As shown in Figures 9 to 12 and in Table 2, the models ability to predict the correct current speed at the correct time and position is not very good (correlation around 0.5). This is as expected, and was also evident in the study in the Sulafjorden area presented in Section 4. For instance the Figures 19 to 22 show similar spread in the scatter plots, indicating bad correlation, whereas the sorted scatter plots and histograms indicate that the statistical distributions for both model and observations are mostly the same for 10 and 25 meters.

Regarding the latter we would like to point the reader to Figure 22 that may be compared to Figures 26 and 28. Both methods, comparing model to SOG-STW and comparing model to ADCP show similar results with regards to spread and statistical distribution. This adds to our impression that the conversion method is useful and thus that the rest of the study presented in Section 3 makes sense. We note that the comparison of model and ADCP has many orders of magnitude more data points than the comparison between model and SOG-STW. One could argue that ADCP data comparison should be limited to the time periods for when the ship passed through the same area as the moorings, but this was not done. A more thorough analysis that goes deeper into the data and tries to quantify, e.g., geographical differences, should also be done. It is possible that there are areas of more predictable currents where the model performs better than other places. More work on this data may unveil these areas, and identify them for those who, e.g., wants to do routing of ships based on the NorKyst800 model.

6 Summary

We have used available data from the ship Samskip Kvitbjørn, that is, primitive data like the *speed through water* (STW), *speed over ground* (SOG), and course and position, to compare modeled currents from the ocean model NorKyst800 with traditional ship observations. Since such ship data is not a measure of the true current, a method whereby the ship data may be converted into true currents is presented as well. The fact that the statistical distributions of both the observations and the modeled current speed are very similar suggests that the method is useful. To investigate the quality of the NorKyst800 model, and the proposed comparison method, we have also included a more traditional comparison in which both model output and ship observations from Samskip Kvitjørn were compared with data from ADCP moorings for a fjord system in the north-western part of Norway. Consequently a part of the analysis is limited to the same geographical area where the ADCP moorings were located. This comparison shows the statistical distribution of the modeled current speed, the observed current speed from the ship (SOG-STW), and the ADCP moorings are all similar. This in turn suggests that primitive ship data are useful data whereby the quality of ocean modeled currents may be assessed and evaluated.

We therefore conclude that the presented method potentially gives us access to a large pool of hitherto unused "ships of opportunity" data which are useful to estimate the quality of the near surface currents of our ocean models. However, this requires that the user is aware of, and understands, the possible sources of errors in the proposed method, and also its limited degree of accuracy.

Acknowledgements

The work was part of the Research Council of Norway IPN MAROFF-programme project grant 282385. We want to thank Birgit Kjoss Lynge (Kongsberg Maritime) for her effort as project leader, and Leif Aarseth and Are Folkestad (Kongsberg Maritime) for their effort in preparing the ship data that was used in this report. We had many great discussions with Birgit, Leif and Are throughout the project that was very valuable to us. We also give a big thanks to Lars Petter Røed (MET Norway) for his work as internal reviewer for this report. In addiction we thank the E39-project for making ADCP-data from moorings in Sulafjorden available.

References

Albretsen, J., and L. Asplin (2021), Hvilken betydning har oppløsning for kyst- og fjordmodeller? Validering og representasjonsberegninger av strømmodeller med eksempler fra Sulafjorden, Møre og Romsdal., *Tech. Rep. Rapport fra havforskningen 20/2021*, Institute of Marine Research, Pb. 1870 Nordnes, N-5817 Bergen, Norway.

Albretsen, J., A. K. Sperrevik, A. Staalstrøm, A. D. Sandvik, F. Vikebø, and L. C. Asplin (2011), NorKyst-800 Report No. 1: User Manual and Technical Descriptions, *Tech. Rep. Fisken og Havet 2/2011*, Institute of Marine Research, Pb. 1870 Nordnes, N-5817 Bergen, Norway.

Furevik, B. R., H. Ágústsson, A. L. Borg, M. Zakari, F. Nyhammer, and M. Gausen (2020), Meteorological observations in tall masts for mapping of atmospheric flow in Norwegian fjords, *Earth System Science Data*, doi:10.5194/essd-2020-32.

Harstveit, K., H. Ágústsson, R. E. Bredesen, B. Furevik, O. J. Aarnes, and J. Albretsen (2018), Sulafjorden og Vartdalsfjorden, Møre og Romsdal. Analyse av modellert vind, strøm og bølger for 2007-2017, *Research Report KVT/KH/2018/R0105*, Kjeller Vindteknikk.

Appendix

A Detailed maps

The following pages offers more detailed versions of the maps in Figure 14 and 15 dividing the Norwegian coast into smaller sections.

Skagerrak east of Lindesnes

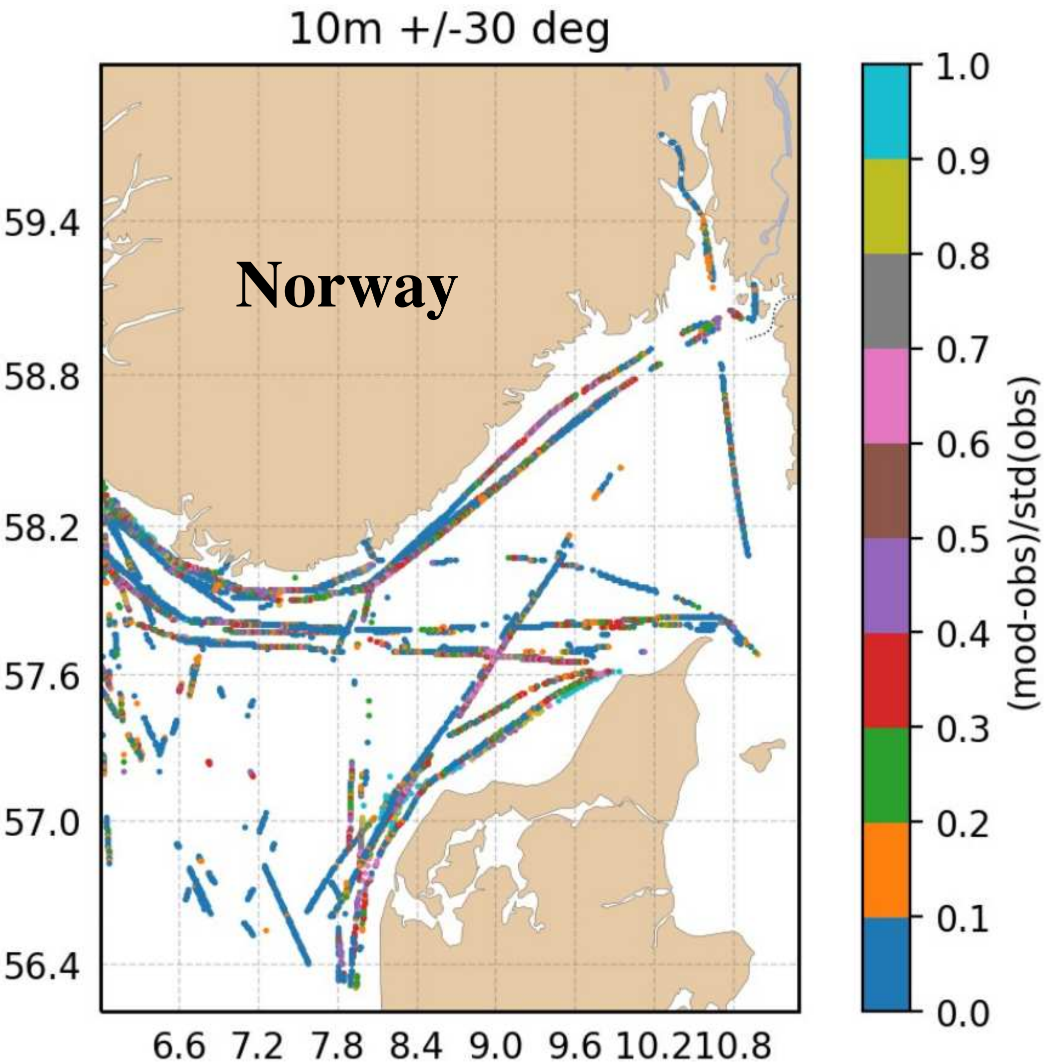

Figure 29: Same as Figure 14, but zoomed in on the area Skagerrak east of Lindesnes.

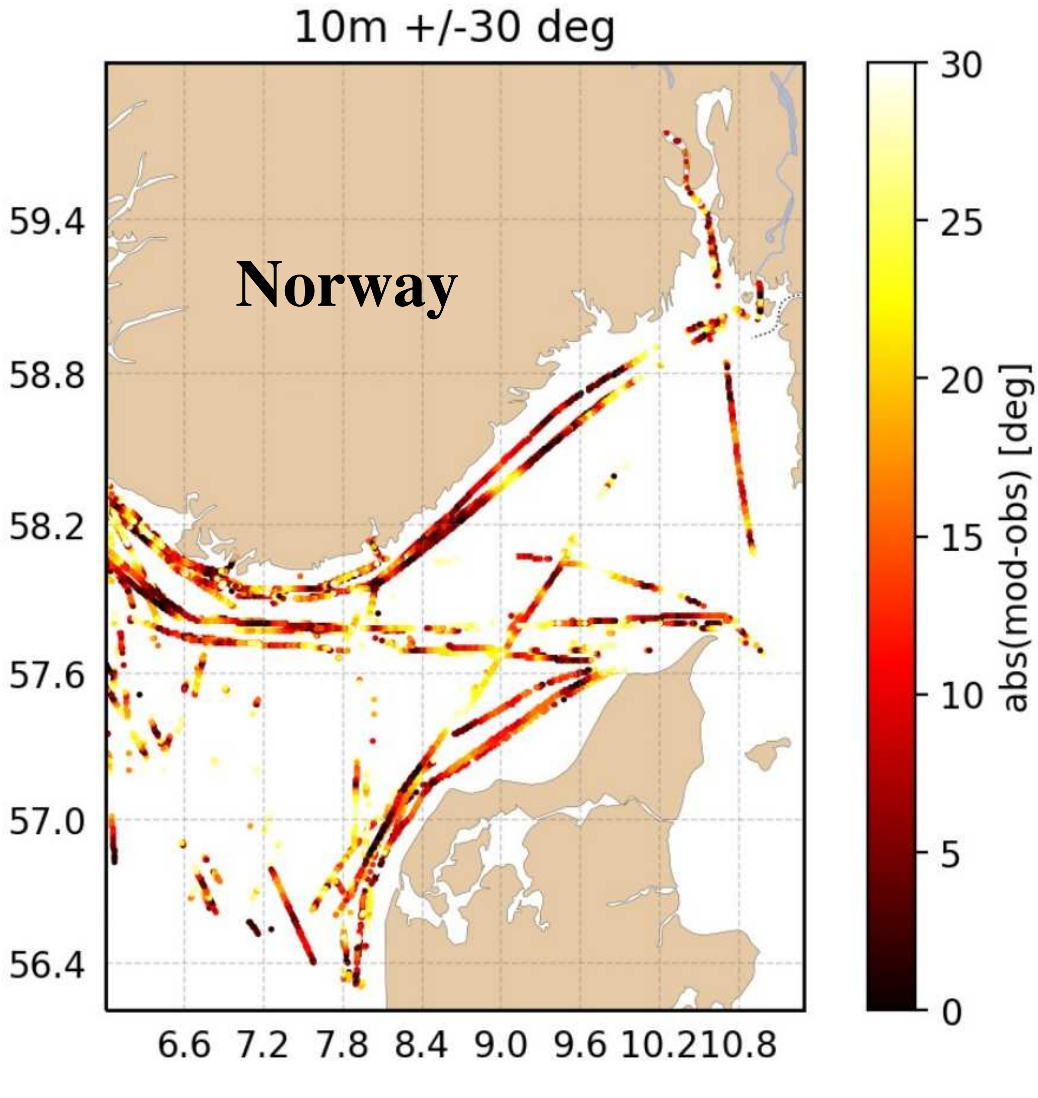

Figure 30: Same as Figure 15, but zoomed in on the area Skagerrak east of Lindesnes.

Lindesnes-Stad

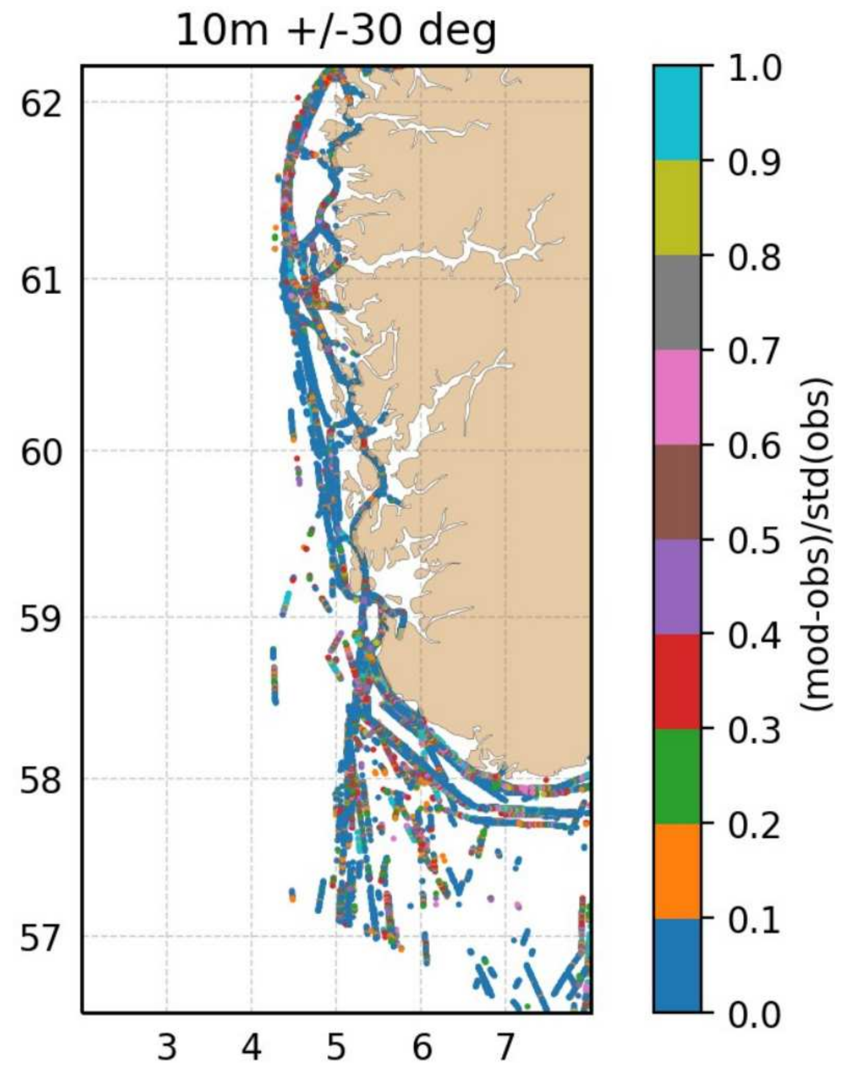

Figure 31: Same as Figure 14, but zoomed in on the area Lindesnes and Stad.

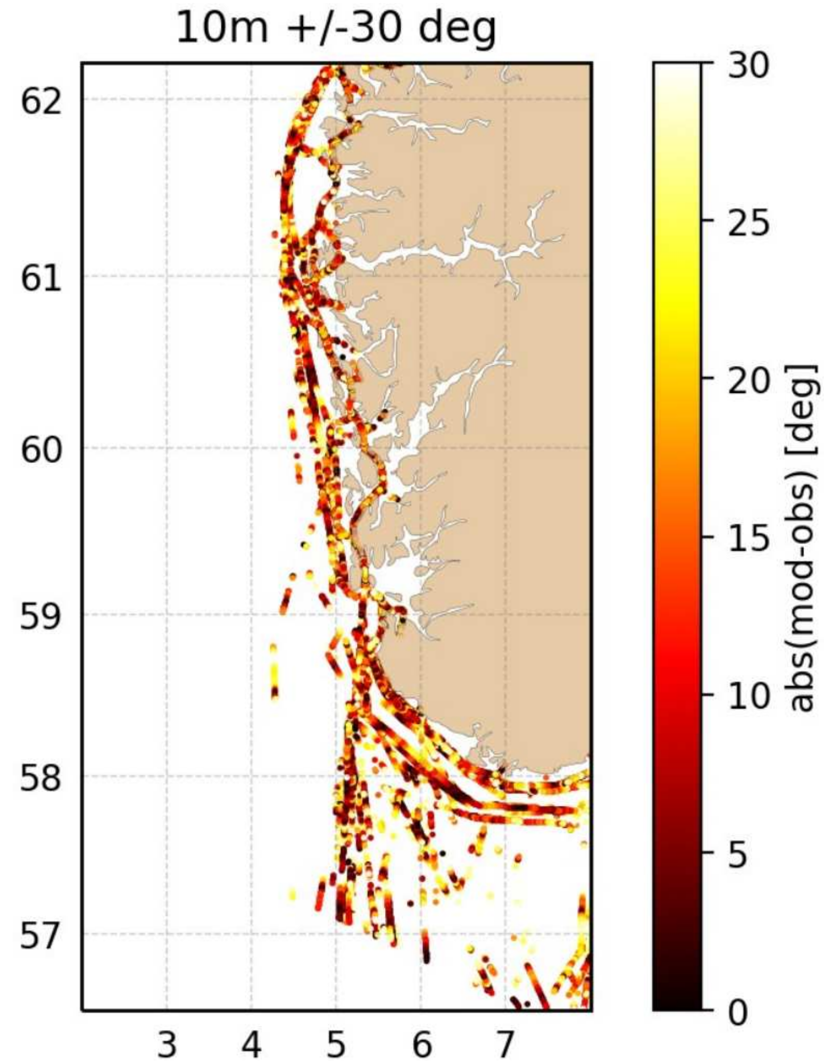

Figure 32: Same as Figure 15, but zoomed in on the area Lindesnes and Stad.

Stad-Bodø

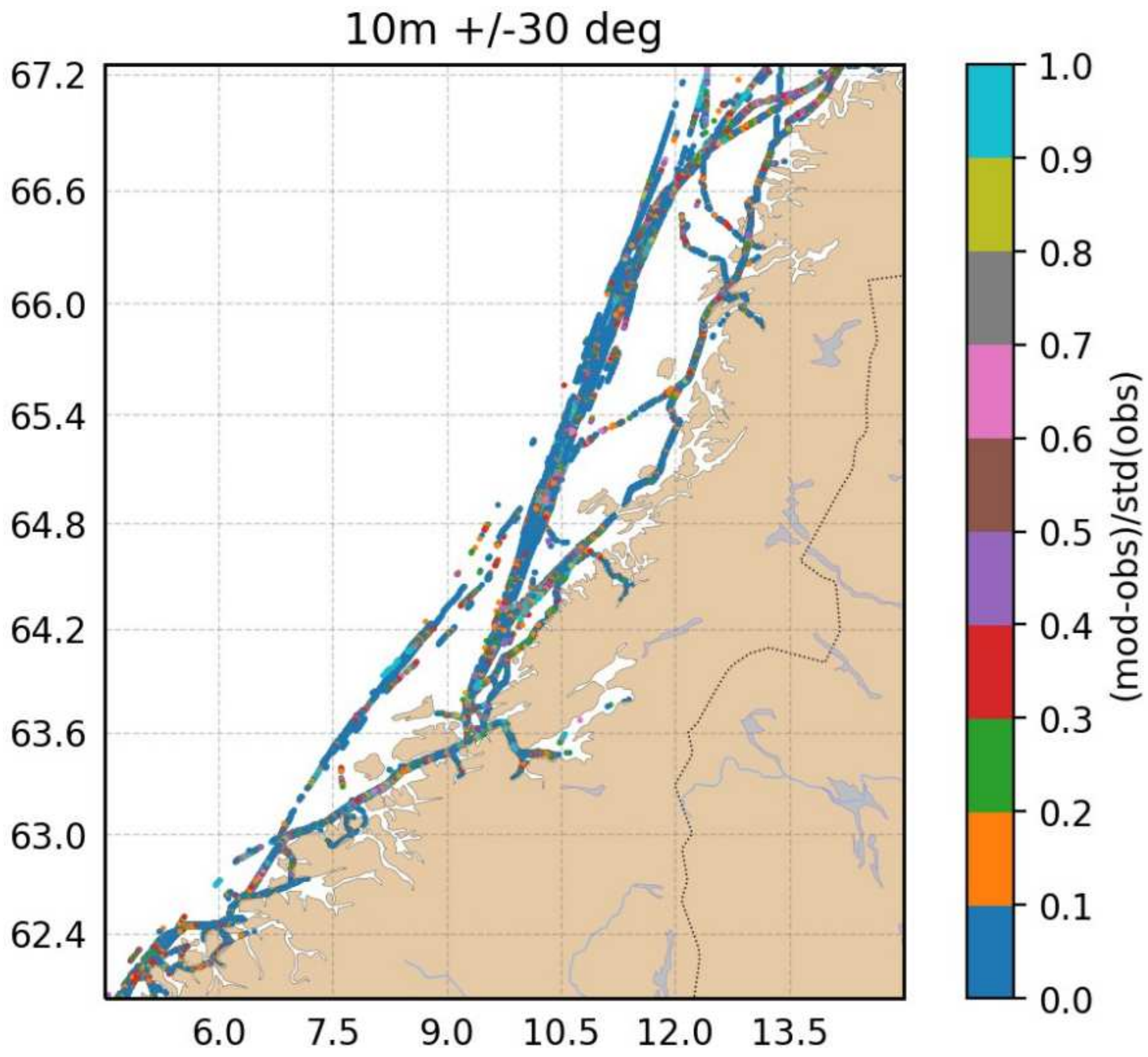

Figure 33: Same as Figure 14, but zoomed in on the area between Stad and Bodø.

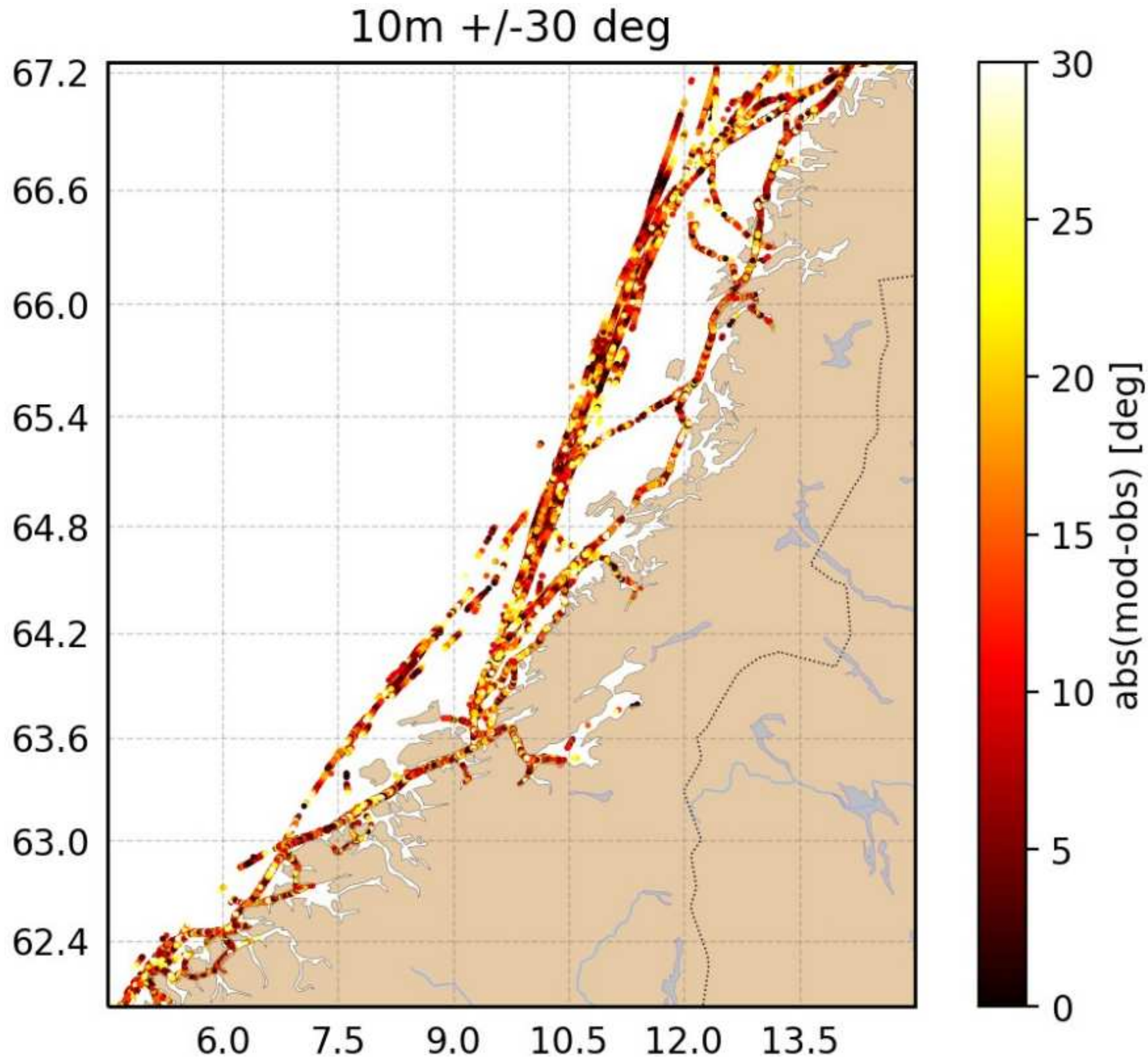

Figure 34: Same as Figure 15, but zoomed in on the area between Stad and Bodø.

North of Bodø

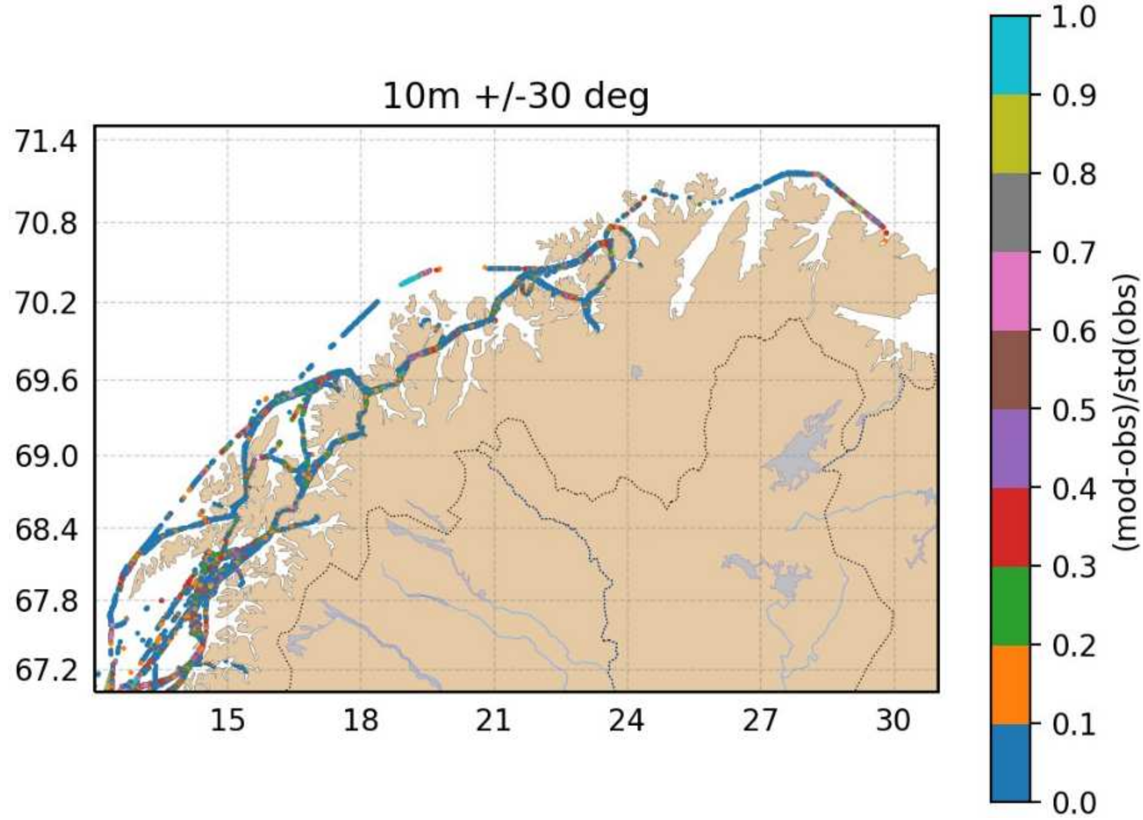

Figure 35: Same as Figure 14, but zoomed in on the area North of Bodø.

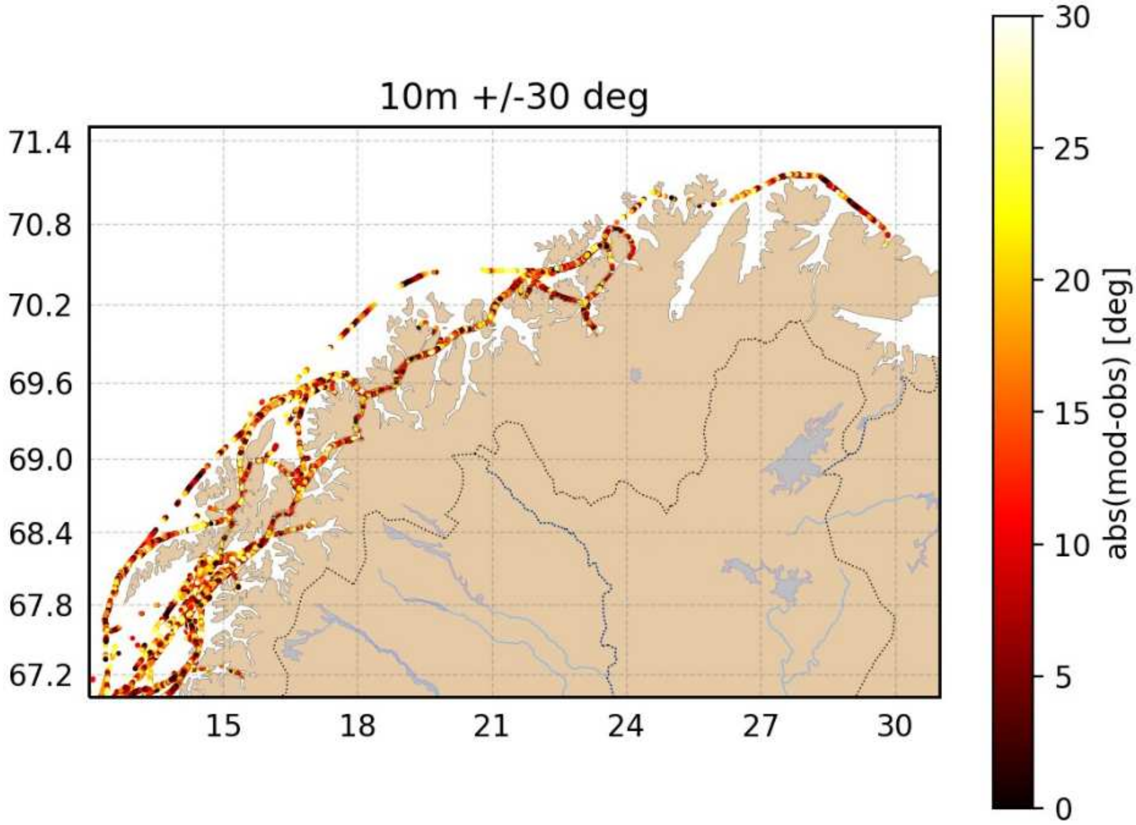

Figure 36: Same as Figure 15, but zoomed in on the area North of Bodø.